

Syracuse University

SURFACE

Dissertations - ALL

SURFACE

June 2015

Influence of environment on soil carbonate clumped isotope records, Andean piedmont of Central Argentina (32-34°S)

Mallory Cecile Ringham
Syracuse University

Follow this and additional works at: <https://surface.syr.edu/etd>



Part of the [Physical Sciences and Mathematics Commons](#)

Recommended Citation

Ringham, Mallory Cecile, "Influence of environment on soil carbonate clumped isotope records, Andean piedmont of Central Argentina (32-34°S)" (2015). *Dissertations - ALL*. 284.
<https://surface.syr.edu/etd/284>

This Thesis is brought to you for free and open access by the SURFACE at SURFACE. It has been accepted for inclusion in Dissertations - ALL by an authorized administrator of SURFACE. For more information, please contact surface@syr.edu.

Abstract

The clumped isotope geothermometer estimates the formation temperature ($T(\Delta_{47})$) of carbonates and has tremendous potential to enhance the extraction of environmental data from pedogenic (soil) carbonate in the geologic record. However, the interpretation of pedogenic carbonate $T(\Delta_{47})$ data is limited by uncertainties in our understanding of carbonate formation processes. This study examines the potential for along-strike, same elevation and plant biomass (C_3/C_4) site variability to influence pedogenic carbonate $T(\Delta_{47})$ data. Pedogenic carbonates were collected from five modern soil pits in the semi-arid eastern Andean piedmont of Argentina under a summer precipitation regime. Three of the five soil pits were instrumented with soil temperature and soil moisture sensors to a depth of 1 m (at 1 km elevation), while a fourth was instrumented with an additional soil CO_2 sensor and atmospheric sensors (temperature, relative humidity, insolation and rainfall) (at 0.6 km elevation). $T(\Delta_{47})$ values are statistically indistinguishable between the four instrumented sites and are invariant with depth. The mean $T(\Delta_{47})$ is $31^\circ C \pm 4^\circ C$ ($\pm 1SE$), reflecting summer soil temperatures. Soil moisture and temperature data indicate that isothermal conditions are achieved immediately after significant wetting events. Carbonate formation under these conditions could result in our observed hot isothermal $T(\Delta_{47})$ values. The results of this study constrain carbonate formation to the early part of soil drying, with $T(\Delta_{47})$ interpretations biased to soil conditions just after major precipitation events.

**INFLUENCE OF ENVIRONMENT ON SOIL CARBONATE CLUMPED ISOTOPE
RECORDS, ANDEAN PIEDMONT OF CENTRAL ARGENTINA (32-34°S)**

By

Mallory Ringham
B.S. Syracuse University, Syracuse, NY 2013

Submitted in partial fulfillment of the requirements for the degree of Master of Science in Earth
Sciences in the Graduate School of Syracuse University

June 2015

Copyright © Mallory Ringham 2015

All Rights Reserved

Acknowledgements

I would like to thank my advisor, Dr. Greg Hoke, for his advice and support throughout an excellent research opportunity involving unique challenges in field work, lab work, and modeling projects. Besides the academics, I am grateful to Greg for stick shift lessons in the middle of the desert (okay, and in the middle of Mendoza, too), for endless Spanish translation services, and for introducing me to Chile's greatest copao shakes. I would also like to thank the members of my committee, Dr. Katherine Huntington and Dr. Christopher Junium, for their guidance on this project, as well as Andy Schauer and Kyle Samek, for providing a great deal of cheerful lab assistance. I would like to thank Julieta Aranibar for above-and-beyond assistance in the field over the past two years. I am indebted to Almendra Brasca for a great few days in the field, involving a continuous game of charades, so much mate, and that time she prevented us both from falling into a ravine. Park rangers at the Villavicencio, Divisadero Largo, and Nacuñan Nature Reserves in the Province of Mendoza were instrumental to this research in selecting, accessing, and building field monitoring stations. And finally, thank you to my family and friends for their love and encouragement, especially to my brother Dale Ringham, for the million and a half times I called to ask "just a really quick Matlab question."

Table of Contents

Abstract	i
Acknowledgements	iv
Table of Contents	v
 Influence of environment on soil carbonate clumped isotope records, Andean piedmont of Central Argentina (32-34°S)	
1. Introduction	1
2. Background	2
2.1 Carbonate Formation.....	2
2.2 General site description.....	5
3. Methods	7
3.1 Field stations and sampling.....	7
3.2 Isotopic methods.....	10
3.3 Carbonate saturation modeling.....	11
4. Results	12
4.1 <i>In situ</i> results.....	12
4.2 Isotopic results.....	16
4.3 Carbonate saturation modeling results.....	20
5. Discussion	20
5.1 Potential for variability in $T(\Delta_{47})$ between sites.....	20
5.2 Invariance of $T(\Delta_{47})$ with depth.....	21
5.3 Isothermal conditions after rainfall events.....	22
5.4 Seasonal controls on soil carbonate $T(\Delta_{47})$	25
5.5 Implications for isotopic records from pedogenic carbonates.....	27
5.6 Recommendations for future work.....	28
6. Conclusions	29
Appendices	30
A <i>In situ</i> site data.....	30
B Summary of all isotopic analyses.....	34
References	38
Vita	43

List of Figures

<i>Figure 1:</i> Site map.....	6
<i>Figure 2:</i> Sensor schematics.....	10
<i>Figure 3:</i> <i>In-situ</i> soil temperature data.....	14
<i>Figure 4:</i> Calculated α_{calcite} values for Nacuñan.....	16
<i>Figure 5:</i> Soil carbonate isotope data.....	19
<i>Figure 6:</i> <i>In situ</i> station records overlaid with $T(\Delta_{47})$ and soil moisture.....	24
.....	
<i>Figure A1:</i> Average daily CAN01 sensor data, July 2013- May 2015.....	30
<i>Figure A2:</i> Average daily CAN02 sensor data, July 2013- May 2015.....	31
<i>Figure A3:</i> Average daily DL01 sensor data, August 2013- May 2015.....	32
<i>Figure A4:</i> Average daily Nacuñan sensor data, July 2013- May 2014.....	33

List of Tables

<i>Table 1:</i> Soil pit and meteorological station locations.....	9
<i>Table 2:</i> Vegetation description	9
<i>Table 3:</i> Summary of isotopic analyses for carbonate samples.....	18
.....	
<i>Table B1:</i> Summary for all replicates of isotopic analyses for carbonate samples.....	34
<i>Table B2:</i> Statistical comparison of $T(\Delta_{47})$ values.....	37

1. Introduction

The development of low temperature geothermometers is important to researchers studying Earth surface processes, paleoaltimetry, and paleoclimate. The clumped isotope geothermometer allows for the determination of near-surface temperatures based on the relative degree of ^{13}C - ^{18}O bonding in carbonates (CaCO_3). "Clumping" of these heavy isotope bonds varies inversely with temperature, providing an estimate of pedogenic carbonate formation temperature ($T(\Delta_{47})$) that is independent of bulk isotopic composition (Ghosh et al. 2006a). Thus, clumped isotopes solve the issue of two unknowns in conventional stable isotope analysis of carbonate, in which the value of $\delta^{18}\text{O}_{\text{soil water}}$ depends on both the temperature of formation and the oxygen isotopic composition of the source water (e.g. Kim and O'Neil, 1997). Previously, calculating $\delta^{18}\text{O}_{\text{sw}}$ values from conventional isotopic analysis of pedogenic carbonate required an assumption about one or the other of these factors, usually temperature.

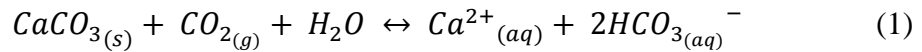
Pedogenic (soil) carbonate is an attractive geologic proxy material because it is commonly present in terrestrial sedimentary rocks. Early uses of clumped isotope geothermometry assumed that pedogenic carbonate formation temperatures reflect mean annual soil temperatures (MAST), with potential systematic errors due to seasonal biases in carbonate formation (e.g. Ghosh et al., 2006b). Breecker et al. (2009) calculated a strong seasonal bias for pedogenic carbonate during warm, drying episodes in the soil when CO_2 concentrations are low in the soil. Several studies have found $T(\Delta_{47})$ far in excess of MAST (e.g. Passey et al. 2010; Quade et al. 2013; Hough et al. 2014) or a mixture of carbonate $T(\Delta_{47})$ data reflecting summer and fall temperatures depending on the timing of the wet season and snowmelt (Peters et al. 2013). Together these data call into question our collective understanding of the process of carbonate formation in the soil profile. This study examines the potential for variability of $T(\Delta_{47})$

data from modern soil carbonates collected in the Andean Piedmont of Argentina (between 32.5 and 34°S; Fig. 1) in order to better constrain the conditions that lead to the formation of soil carbonate and to improve interpretations of clumped isotope paleoenvironmental records. We simplified our investigation by (1) choosing sites in a summer-only precipitation regime, thereby limiting variability in seasonal soil drying periods, (2) varying C₄/C₃ grass proportions, which may bias seasonal soil moisture and CO₂ conditions during times of peak productivity, and (3) comparing nearby sites at a single elevation, as some studies show a strong correlation between T(Δ₄₇) and elevation (Quade et al 2013; Hough et al. 2014) while others do not (Peters et al. 2013). Our objectives are to (1) explore the influence of environmental variables (air temperature, soil temperature, soil moisture, soil gas CO₂ concentration and vegetation type via *in-situ* monitoring) on the timing and temperature of pedogenic carbonate formation, and (2) determine the potential for site-to-site variability in resulting T(Δ₄₇) values.

2. Background

2.1 Carbonate Formation

Pedogenic carbonate forms over hundreds to thousands of years as filaments, then nodules in sub-humid to arid soils when the soil solution becomes supersaturated with calcite (Cerling and Quade, 1993). The carbonate formation reaction,



and its corresponding activity equation under aqueous conditions,

$$\alpha_{CaCO_3} = \frac{4m^3_{Ca^{2+}}}{pCO_2} \left(\frac{K_2}{K_1 K_{cal} K_{CO_2}} \right) \quad (2)$$

show that carbonate precipitation in soils may result from any one or a combination of the following: an increase in soil temperature, a decrease in soil gas pCO₂, or an increase in Ca²⁺ or

HCO_3^- concentration in solution (Breecker et al., 2009). In well-drained, arid climate soils, carbonate formation should occur during periods of soil dewatering, due to evaporation and root uptake that begins immediately after precipitation events. Carbon in pedogenic carbonates (from soil CO_2 from plant root and microbial respiration) is depleted in ^{13}C relative to atmospheric CO_2 , with a positive shift in $\delta^{13}\text{C}$ near the surface caused by atmospheric exchange (Cerling and Quade, 1993). $\delta^{18}\text{O}_{\text{carbonate}}$ depends on $\delta^{18}\text{O}_{\text{soil water}}$ and temperature-dependent fractionation during carbonate formation. In well-drained soils, $\delta^{18}\text{O}_{\text{soil water}}$ is commonly assumed to reflect meteoric water, and is typically enriched near the surface by evaporation (e.g. Cerling and Quade, 1993). In equation 2, $p\text{CO}_2$ is the partial pressure of carbon dioxide in the soil gas, $m_{\text{Ca}^{2+}}$ is the calcium ion concentration in the soil solution (provided by rainwater and dissolution of Ca-bearing minerals in dust or soil parent material), and K values are temperature-sensitive equilibrium constants as described by Drever (1982) and Plummer and Busenberg (1982). An activity of calcite (α_{CaCO_3}) > 1 indicates precipitation of CaCO_3 . This equation is valid for systems under conditions of thermodynamic equilibrium where activity \approx concentration and soil water $\text{pH} \leq 9$. In theory, isotopic equilibrium of pedogenic carbonate with soil CO_2 and soil water is reached during drying episodes and is due to the slow precipitation of calcite at depth in soils (Breecker et al. 2009; Cerling and Quade, 1993). However, recent studies have suggested that isotopic equilibrium in soil carbonate formation is not always achieved (Gabitov et al., 2012). Isotopic disequilibrium effects may result in decreased Δ_{47} measurements, artificially raising $T(\Delta_{47})$ values (Guo 2008).

Quade et al. (2013) found that average clumped isotope $T(\Delta_{47})$ measurements of modern soil and paleosol carbonates from soils typically developed under summer rainfall seasonality reflect the hottest months of the year, exceeding the mean annual air temperature (MAAT) by

10-15°C. This study suggested that an increase in reported $T(\Delta_{47})$ values towards the surface may be due to radiative heating of the soil; however $T(\Delta_{47})$ values considered with typical uncertainties appear to be isothermal with depth. Passey et al. (2010) found that temperatures recorded by modern soil carbonates in East Africa exceeded present-day MAST, plotting closely with the average summer soil temperatures. Peters et al. (2013), investigated seasonal bias on carbonate formation temperatures along an elevation transect in the central Andes at ~33°S and found that average $T(\Delta_{47})$ values for carbonates collected above 2 km elevation reflect summer soil temperatures, while those below 2 km more closely reflect MAST. This transition coincides with a change in seasonality of precipitation, with winter precipitation above 2 km elevation and summer precipitation below. Peters et al. (2013) suggested that below 2 km, summer rainfall delays soil drying until fall, resulting in carbonate formation later in the year recording cooler $T(\Delta_{47})$ values. Above 2 km and in winter-only precipitation regimes, soil should dry during the warmest months, allowing for carbonate formation with summer $T(\Delta_{47})$.

The type and amount of vegetation in a region may also influence the timing and temperature of carbonate formation because plants impact the radiative heating of the soil surface and focus removal of moisture within the rooted part of the soil profile. C_3 and C_4 type plants are adapted to different levels of CO_2 , light intensity, and water stress due to variations in their metabolic pathways for photosynthetic carbon fixation. C_3 plants are adapted to be most productive under moderate soil and air temperatures and light intensities; in arid environments, C_3 plants are most active during spring and fall. C_4 plants, including most grasses in arid regions, are generally adapted to higher water stress (dry) conditions with low CO_2 concentrations. C_4 plants are most productive during the hottest months of the year and enhance soil dewatering

during this time, so it is expected that carbonate $T(\Delta_{47})$ values will be higher in regions with significant C_4 plant distributions than in regions with C_3 vegetation (Breecker et al. 2009).

2.2 General sampling site description

We sampled pedogenic carbonate from the eastern Andean piedmont of Argentina at 32-34°S in the Villavicencio (CAN01, CAN02), Divisadero Largo (DL01), and Nacuñan Nature Reserves (Figure 1). The piedmont is an arid, gently eastward sloping topographic feature; the western edge borders the Andes at ~1000 m elevation, sloping down to the eastern edge at an elevation of ~500 m. The entire piedmont experiences spatially discontinuous summer convective precipitation with infrequent westerly precipitation events rarely reaching its western edge during the winter months (Mancini et al., 2005). Mean annual air temperature recorded at Mendoza (827 m elevation) is ~17 °C and mean annual precipitation is ~220 mm (1989-2015) from Base de Datos Hidrológica Integrada (BDHI; <http://bdhi.hidricosargentina.gov.ar>); Servicio Meteorológico Nacional (SMN; <http://www.smn.gov.ar>). Surveys of vegetation type and cover density across the piedmont reveal a nearly 50/50 C_4/C_3 grass mixture at 1000 m elevation in the west evolving to a 90/10 mixture at 600 m in the east (Cavagnaro, 1988). At higher elevations, genus *Larrea* shrubs dominate, and the size and density of shrubs and trees increases to the east. Soils of the western piedmont are developed in a coarse-grained alluvial conglomerate parent material and contain stage I/II carbonate development (Gile et al. 1966; Birkeland, 1999). Terrestrial cosmogenic nuclide dating by Schmidt et al. (2011) between the Villavicencio Nature Reserve and the City of Mendoza yielded terrace ages between 21 and 0.7 ka on adjacent, tectonically uplifted surfaces.

The Nacuñan Nature Reserve is located ~150 km to the southeast of Mendoza at 34 °S. This region also experiences summer-only precipitation, with an average annual precipitation of ~326 mm and a mean annual air temperature of ~16 °C (Ojeda et al. 1998). Plant productivity here is higher than Villavicencio and Divisadero Largo sites, though total C₄/C₃ distribution (grasses and shrubs) is similar to Villavicencio. The soil parent material is medium to coarse grained sand that contains carbonate nodules. The soil is modern, based on radiocarbon dating of carbonate nodule samples (Section 3.1).

Prior work in this region documents the elevation dependence of $\delta^{18}\text{O}$ values in precipitation, river water, and pedogenic carbonate over a ~100 km E-W transect that crosses the Andes through the Río Mendoza valley (Hoke et al. 2009; 2013). Peters et al. (2013) investigated soil carbonate formation and associated clumped isotope records through the Río Mendoza transect; data from their 2 nearest sites are provided for comparison with our data (Figures 1,3,5,7).

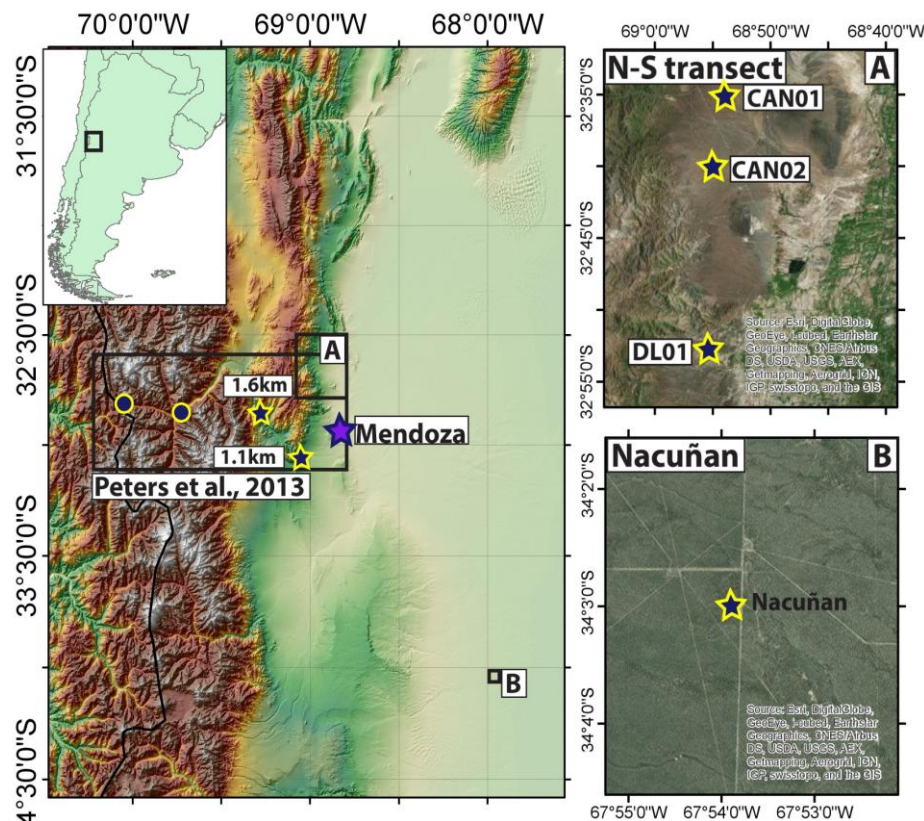


Figure 1:
Eastern Andean
piedmont of central
Argentina, 32-34°S.

Left: Peters et al. 2013
transect with
subsurface monitoring
sites at 3.2 km, 2.40
km, 1.6 km and 1.1
km.

Right: Inset A:
locations of CAN01,
CAN02, and DL01
subsurface monitoring
sites. Inset B: location
of Nacuñan Nature
Reserve site.

3. Methods

3.1 Field Stations and Sampling

In order to investigate the impact of seasonality on soil carbonate growth and recorded $T(\Delta_{47})$, we collected *in situ* field data on subsurface conditions (soil temperature, soil moisture, CO₂ concentration, rooting depth, substrate, carbonate stage) and meteorological conditions (air temperature, rainfall, relative humidity, insolation). Vegetation data is based on a point intercept survey conducted in a representative, undisturbed area near the pits at the end of the study in April-May 2015, with biomass estimated as % cover. In July 2013, four pits were excavated at sites over a ~40 km N-S transect between the Villavicencio Nature Reserve and the Divisadero Largo Nature Reserve (~32.7°S) (see Figure 1, Table 1). Two pits (CAN01 and CAN02), separated by ~6 km, were instrumented with Onset soil temperature sensors (10, 50, and 100 cm), and soil moisture sensors (50 cm) connected to an Onset microstation data logger (Figure 2a). A pendant temperature logger mounted in a radiation shield was suspended from a pole at a height of 1.5 m above the ground surface. A third pit (DL01) was instrumented with a microstation data logger and soil temperature and moisture sensors at 10 and 50 cm depth. Stage I-II soil carbonate clasts were collected at these sites at 15-20 cm intervals from the first occurrence of carbonate to 1m depth. Carbonate clasts collected at 40cm depth in DL01 were analyzed for radiocarbon age through DirectAMS. The fourth pit (CAN03) was excavated to a depth of 50 cm and sampled for carbonate clasts at that same depth. The substrate for each of these soil pits is cobble to boulder conglomerate. A fifth pit was sampled for carbonate nodules to 1m depth at 34°S in the Nacuñan Nature Reserve (Figure 1, Table 1). Carbonate nodules collected at 30, 50, and 100 cm depth were analyzed for radiocarbon dating at DirectAMS. This pit was instrumented with Onset soil moisture and temperature sensors at 10, 50, and 100 cm

depth, a Vaisala pCO₂ sensor at 50 cm depth, and Onset air temperature, relative humidity, insolation, and rain sensors (Figure 2b). Readings from all of the instruments were logged at 15 minute intervals by an Onset U30-NRC logger; all sensors were tested prior to deployment in the field for proper functionality, and resulting data were calibrated according to the manufacturer.

CAN01 and CAN02 lie in a mixed C₄/C₃ vegetation environment dominated by C₃ plants with a C₄ grass layer (Table 2). DL01 was dominated by C₃ grasses and shrubs with a much higher plant cover than the previous sites. The high biomass and dominance of C₃ at this site may be caused by the slight southern aspect of this terrace, which receives lower irradiance than the more exposed CAN01 and CAN02. Nacuñan lies in a mixed C₄/C₃ vegetation environment with the highest productivity of the four sites, including a dominantly C₄ grass layer and a high density of C₃ shrubs.

Daily precipitation data are available from BDHI for stations Mendoza Airport (near CAN01 and CAN02), and for San Rafael (<100 km southwest of Nacuñan). Daily air temperature and precipitation data are also available for NOAA's National Climatic Data Center (NCDC) (<http://www.ncdc.noaa.gov/>) at Mendoza Airport and Mendoza Observatory. Limited daily air temperature, precipitation amount, and δ²H and δ¹⁸O data are available for Mendoza Observatory and Nacuñan through the Global Network of Isotopes in Precipitations (GNIP) (http://www.naweb.iaea.org/napc/ih/IHS_resources_gnip.html) and Hoke et al. (2013).

Table 1: Soil pit and meteorological station locations

Soil pit site:	Location		Elevation	Data available
	Latitude (S)	Longitude (W)	(m)	
CAN01	32° 35' 31"	68° 54' 19"	~1000	Soil T (10, 50, 100 cm), Soil Moisture (50 cm), Carbonate clasts collected to 1m depth
CAN02	32° 39' 07"	68° 55' 00"	~1000	Soil T (10, 50, 100 cm), Soil Moisture (50 cm) Carbonate clasts collected to 1m depth
CAN03	32° 34' 12"	68° 56' 34"	~1000	No instrumental data, Carbonate clasts collected at 50 cm depth
DL01	32° 52' 40"	68° 55' 21"	~1000	Soil T (10, 50 cm), Soil Moisture (10, 50 cm) Carbonate clasts collected to 1m depth
Nacuñan	34° 02' 60"	67° 54' 10"	~540	Soil T (10, 50, 100 cm), Soil Moisture (10, 50, 100 cm), CO ₂ (50 cm), Air T, Precip., Insolation, Carbonate nodules collected to 1 m depth
Peters et al. 2013 (1.1 km)	33° 02' 38"	69° 00' 33"	~1100	Soil T (10, 50, 100 cm), Soil Moisture (50 cm), Carbonate clasts collected to 1m depth
Peters et al. 2013 (1.6 k)	32° 49' 24"	69° 17' 55"	~1600	Soil T (10, 50, 100 cm), Soil Moisture (50 cm), Carbonate clasts collected to 1m depth
Meteorological station:	Latitude (S)	Longitude (W)	Elevation	Data available
BDHI: Mendoza	33° 00' 54"	69° 07' 03"	~1000	Precip. (1983-2015)
NCDC: Mendoza Airport	32° 49' 59"	68° 46' 59"	~1000	Air T, precip. (1959-2015)
NCDC: Mendoza Observatory	32° 53' 00"	68° 51' 00"	~1000	Air T, precip. (1959-2015)
GNIP: Mendoza Observatory	32° 52' 48"	68° 51' 00"	~1000	Air T, precip., $\delta^2\text{H}$, $\delta^{18}\text{O}$ (1982-1988, 1998-1999)
GNIP: Nacuñan	34° 01' 48"	67° 58' 12"	~540	Air T, precip., $\delta^2\text{H}$, $\delta^{18}\text{O}$ (1982-1984)
BDHI: San Rafael	34° 36' 44"	68° 18' 58"	~1000	Precip. (1984-2014)

Table 2: Vegetation description with biomass estimated by % cover

	CAN01	CAN02	DL01	Nacuñan
% bare soil	25	22	3	0
C ₄ / C ₃ grasses	4.80	36.00	0.10	2.80
C ₄ / total vegetation cover	0.32	0.46	0.02	0.42
Dominant grasses (C ₃ or C ₄)	<ul style="list-style-type: none"> •<i>Pappophorum</i> (C₄) •<i>Bouteloa barbata</i> (C₄) •<i>Eragrostis</i> (C₄) 	<ul style="list-style-type: none"> •<i>Pappophorum</i> (C₄) •<i>Bouteloa barbata</i> (C₄) •<i>Eragrostis</i> (C₄) 	<ul style="list-style-type: none"> •<i>Jarava ichu</i> (formerly <i>Stipa ichu</i>) (C₃) 	<ul style="list-style-type: none"> •<i>Pappophorum caespitosum</i> (C₄) •<i>Trichloris crinita</i> (C₄) •<i>Setaria mendocina</i> (C₄) •<i>Jarava ichu</i> (formerly <i>Stipa ichu</i>) (C₃)
Dominant CAM (cacti) (C ₄)	<ul style="list-style-type: none"> •<i>Opuntia</i> (C₄) •<i>Tephrocactus</i> (C₄) 	<ul style="list-style-type: none"> •<i>Opuntia</i> (C₄) •<i>Tephrocactus</i> (C₄) 		
Dominant shrubs (C ₃)	<ul style="list-style-type: none"> •<i>Lycium tenuispinosum</i> •<i>Larrea cuneifolia</i> •<i>Zucagnia punctata</i> 	<ul style="list-style-type: none"> •<i>Lycium tenuispinosum</i> •<i>Larrea cuneifolia</i> •<i>Zucagnia punctata</i> 	<ul style="list-style-type: none"> •<i>Trycicla spinosa</i> •<i>Lycium tenuispinosum</i> •<i>Verbena aspera</i> 	<ul style="list-style-type: none"> •<i>Larrea cuneifolia</i> •<i>Larrea divaricata</i> •<i>Lycium tenuispinosum</i> •<i>Prodopsis flexuosa</i> •<i>Geoffroea decorticans</i>

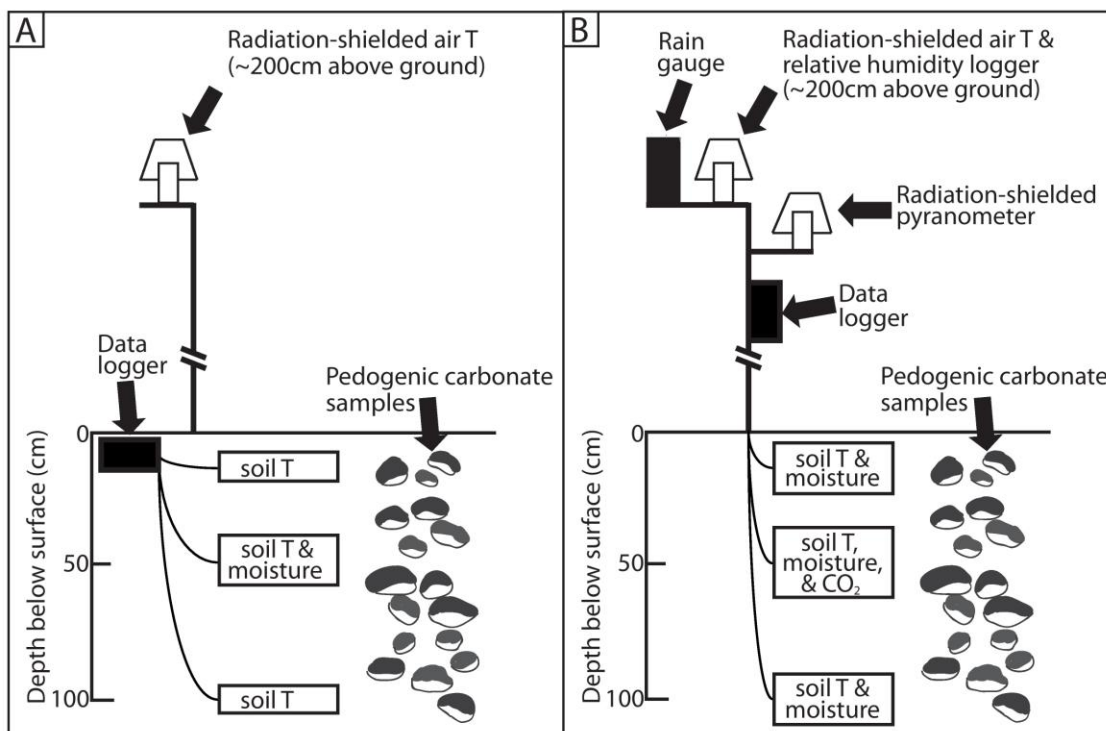


Figure 2: (a) CAN01 and CAN02 site sensor instrumentation (from Peters et al. 2013) (b) Nacuñan soil and atmospheric sensor instrumentation.

3.2 Isotopic methods

Carbonate coatings from rocky, western piedmont samples were scraped from multiple clasts collected at the same depth, powdered, and homogenized with an agate mortar and pestle. Carbonate nodules collected from the sandy soil substrate at Nacuñan were crushed and homogenized, with care taken to remove any roots and obvious organic material. The powdered and homogenized samples were analyzed at the University of Washington's Isolab in December 2013 and July 2014, where they were digested in 105% phosphoric acid at 90°C with the evolved CO₂ gas purified as described in Huntington et al. (2009). Between two and five replicates of each carbonate-derived CO₂ sample were analyzed on a Thermo MAT 253 mass spectrometer, returning measurements of $\delta^{13}\text{C}$, $\delta^{18}\text{O}$, Δ_{47} , and Δ_{48} (used to screen for contaminants.). Experimentally determined mass ratios compare the mass 47 abundance of a CO₂ sample to that

of a stochastic CO₂ standard heated to a known temperature; this sample Δ_{47} is then compared to the absolute reference frame (ARF) (Dennis et al. 2011). $T(\Delta_{47})$ values were calculated using synthetic carbonates calibrations in the ARF (Dennis et al., 2011; Zaarur et al. 2013). For the range of Δ_{47} values reported in this study (0.638-0.706‰, Table 3), the Zaarur and Dennis calibrations result in similar carbonate formation temperature estimates, differing by an average of 8% for samples run with $n = 3$ replicates. $T(\Delta_{47})$ values from samples with $n=3$ replicates are generally recorded to 3-5°C precision (95% confidence). Select samples were also analyzed using a Kiel III carbonate device coupled to a Thermo Delta Plus SIRM for a dual-inlet based $\delta^{13}\text{C}$ and $\delta^{18}\text{O}$ carbonate measurement (noted in Table 3) and reported relative to Vienna PeeDee Belemnite (VPDB).

Peters et al. (2013) samples were reported pre-ARF and are not directly comparable to samples reported in the ARF. Samples from each Peters et al. (2013) site at 50 cm depth were reanalyzed at the University of Washington in April 2015 in the ARF.

3.3 Carbonate saturation modeling

Station measurements from Nacuñan provide the soil temperature and soil CO₂ concentration data necessary to solve equation 2 at 50 cm depth. The concentration of calcium ions in the soil solution of this region is taken to be ~3-4 meq/L (or 1.5-2.0 mmol/L), as measured in surface soils at Nacuñan (0-20 cm depth) (Rossi 2004; Rossi and Villagra 2003). By comparing sensor conditions to calculated activities, we generalize supersaturation conditions and seasonality of carbonate formation.

4. Results

4.1 *In-situ results*

Radiocarbon dating of carbonate clasts collected at 40cm depth in DL01 produced an age of $2080 \pm 30(1\sigma)$ years BP, and nodules collected at 30, 50, and 100 cm depth at Nacuñan produced ages of 5900 ± 30 , 11140 ± 40 , and 16200 ± 70 years BP, respectively, indicating modern carbonate formation. As soil carbonates grow over time, additional ^{14}C is incorporated into coatings or nodules; this time integration results in radiocarbon ages that are typically interpreted as underestimates of the true age of carbonate formation (Amundson et al. 1994; Yang et al. 1994). As such, the Nacuñan radiocarbon signals are consistent with a stable soil pit.

At least 1.5 years of data collected at 15 min. intervals are available for each instrumented soil pit (starting in July 2013). Air temperature data are available at CAN01, CAN02, and Nacuñan. CO_2 soil gas concentration at Nacuñan is available from mid-February 2014 through May 2015; missing data prior to February 2014 was due to a blown fuse in the solar power system for the CO_2 sensor. Other minor gaps in data collection stem from dead batteries at CAN01, excess water in the CAN01 and DL01 microloggers, and rodent activity that damaged sensor cables at DL01 (see Appendix).

Soil temperatures for all 4 pits ranged between 0°C and 40°C for sensors at 10 cm depth and between 8°C and 35°C for sensors at 50 and 100 cm depth. Recorded soil temperatures were comparable for all sites. Soil temperatures for our sites as well as the two nearest Peters et al. (2013) sites are overlain with average $T(\Delta_{47})$ values in Figure 3. For the CAN01, DL01, and Nacuñan stations, $T(\Delta_{47})$ ranges intersected soil temperatures only during the hottest summer months. $T(\Delta_{47})$ values for CAN02 intersect late spring and late summer soil temperatures. Data from Peters et al.'s (2013) 1.1km and 1.6km stations intersected $T(\Delta_{47})$ values at late spring,

early fall, and for a brief period during summer (January 2011). These station data were recorded in 2010 under typical MAAT conditions of 15°C and 13°C, respectively, based on nearby weather stations (Guido and Cachueta), with precipitation for the recorded year falling ~30% below the historical means.

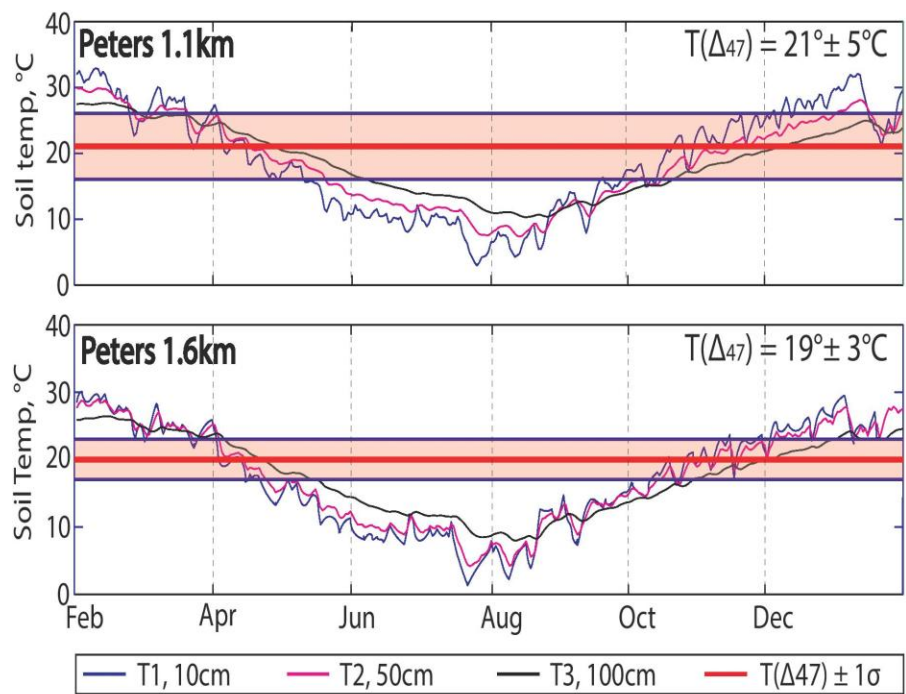
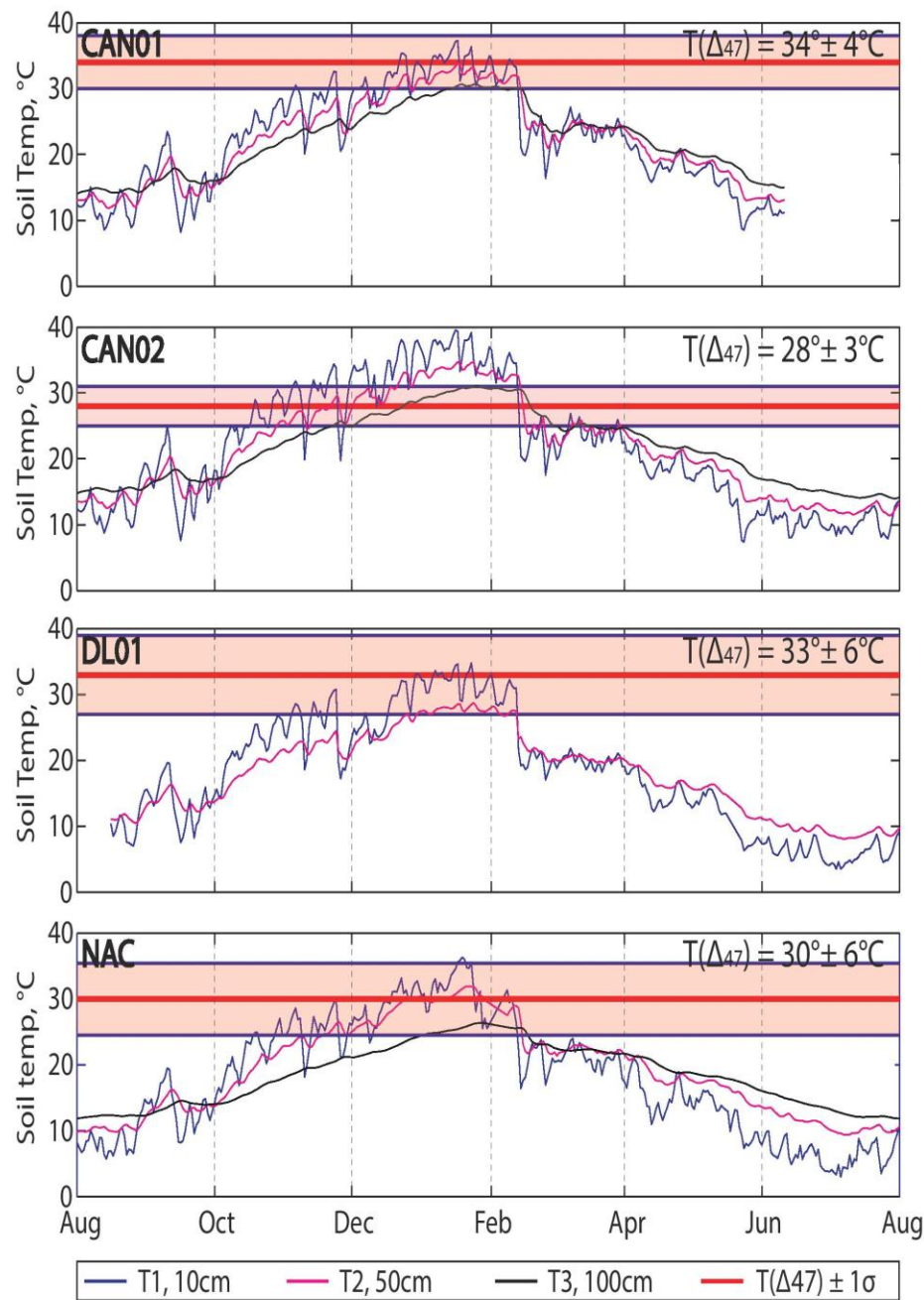


Figure 3: *In-situ* station records averaged daily overlaid with $T(\Delta_{47})$ values for August 2013-August 2014 (*this study*); *in-situ* records and $T(\Delta_{47})$ values for February 2010-January 2011 (*Peters et al., 2013*)

Soil moisture values $<0.10 \text{ m}^3/\text{m}^3$ are "oven dry" to "dry" soils, according to the manufacturer (Onset), though within this regime wetting events can still be identified. Values of $0.30 - 0.50 \text{ m}^3/\text{m}^3$ represent wet to saturated soils. We recorded soil moisture values between 0.00 and $0.30 \text{ m}^3/\text{m}^3$ at 50 cm depth for all sites. A significant soil wetting event was captured at 50 cm depth for all sites in late February 2014, although conditions at CAN02 during this event remained "dry" with a peak soil moisture of $0.09 \text{ m}^3/\text{m}^3$. DL01 captured 4 additional soil wetting events at 50 cm depth, occurring in December 2013, April 2014, and December 2014. Sensors at Nacuñan captured 1 wetting event at 100 cm depth in late February 2014 and a series of wetting events at 50 cm depth in December 2014 - April 2015.

The total precipitation for August 2013 - August 2014 recorded from Mendoza for sites CAN01, CAN02, and DL01 was between 260 (Mendoza Airport) and 280 mm (Mendoza Observatory), exceeding the mean annual precipitation of 220 mm by $\sim 20\%$. The total precipitation for August 2013-August 2014 recorded at Nacuñan by our rain gauge was $\sim 430 \text{ mm}$, exceeding the annual average (Nacuñan GNIP station, $n = 4$) of 326 mm by $\sim 30\%$. Average air temperatures recorded for Mendoza and Nacuñan both reflected the historical MAAT of 17°C and 16°C , respectively, with daily averaged air temperatures recorded between 0°C and 35°C . Solar radiation for Nacuñan ranged between 0 and $\sim 1275 \pm 65 \text{ W/m}^2$, with maximum insolation occurring between December 2013 and March 2014.

The percentage of CO_2 in the soil gas recorded at 50cm depth for Nacuñan ranged between 0.12 and 0.60% between February 2014 and May 2015, with maximum CO_2 concentrations occurring in late February - April 2014. CO_2 concentrations rose sharply in February in the middle of the growing season in response to wetting events (Figure 4).

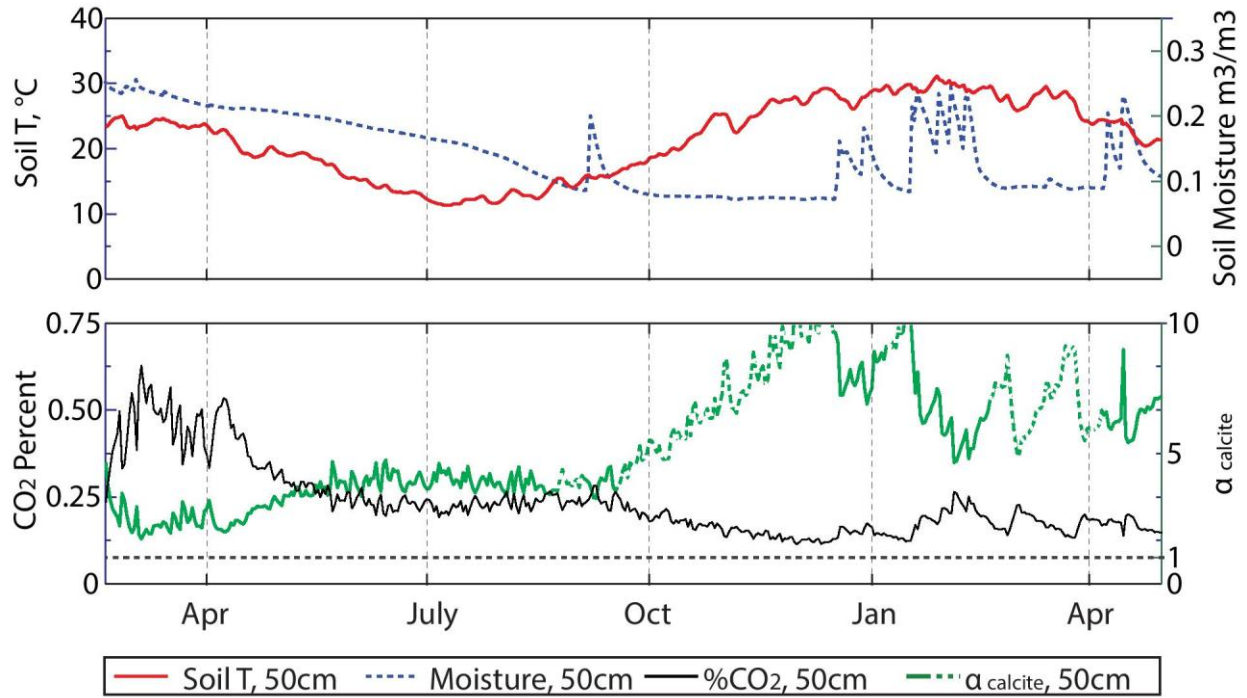


Figure 4: *In-situ* Nacuñan records (soil temperature, soil moisture, and soil gas CO₂ concentration at 50 cm) with calculated α_{calcite} values, mid-February 2014 - May 2015. Solid portions of the α_{calcite} line indicate times when the soil has a moisture content $> 0.1 \text{ m}^3/\text{m}^3$.

4.2 Isotopic results

Isotopic results are summarized in Table 3 and Figure 5. Soil carbonate $\delta^{13}\text{C}$ and $\delta^{18}\text{O}$ measurements generally decrease with depth and range from -6.0 to -0.3‰ (VPDB) and from -8.0 to 2.3‰ (VPDB), respectively. A full summary of replicate measurements is available in the Appendix. At and below 50 cm, the range of $\delta^{13}\text{C}$ values from CAN01, CAN02, CAN03, and DL01 is -6.0‰ to -2.1‰, and the range of $\delta^{18}\text{O}$ values is -8.5‰ to -0.1‰.

Δ_{47} values are reported in the ARF (Dennis et al., 2011) and range between 0.638 and 0.706‰. For all $\Delta_{47} < 0.695$ ‰, $T(\Delta_{47})$ values calculated using Dennis et al. (2011) are slightly warmer than those following Zaarur et al. (2013); however all $T(\Delta_{47})$ values calculated using the two calibrations lie within 1 standard error of one another. $T(\Delta_{47})$ values range between 24°C and 42°C (Zaarur calibration) and between 22°C and 50°C (Dennis calibration). Individual $T(\Delta_{47})$

values in Figure 5 are shown using the Zaarur et al. (2013) calibration. $T(\Delta_{47})$ values from Peters et al. (2013) for the nearest elevation pits (1.1 and 1.6 km) are provided for comparison (Fig. 3); the majority of these data were calculated using Ghosh et al. (2006) and were not reported in the ARF. However, samples at 50 cm depth from the 1.1 and 1.6 km sites were replicated in the ARF, resulting in $T(\Delta_{47})$ differing from pre-ARF values by less than 2°C.

Average $T(\Delta_{47})$ values for all sampled pits vary little with depth. The mean $T(\Delta_{47})$ value for the N-S transect bordering the mountains is $32^{\circ}\text{C} \pm 3^{\circ}\text{C}$ ($\pm 1\text{SE}$) and for Nacuñan is $30^{\circ}\text{C} \pm 3^{\circ}\text{C}$. At all pits, $T(\Delta_{47})$ values exceed MAAT and MAST (Figure 5). Pit-averaged $T(\Delta_{47})$ values are greater than or equal to the average hottest month mean soil temperature (HMST) at 50cm, with the exception of CAN02, which falls between MAST and HMST (Fig. 3). CAN02's $T(\Delta_{47})$ values are slightly cooler than those of CAN01. CAN02 and CAN01, which are separated by ~6 km, have mean $T(\Delta_{47})$ values (33°C and 28°C , respectively) that are statistically different ($T = 3.13$, $P < 0.05$). No other pairings between the four sites exhibited $T(\Delta_{47})$ values that were statistically different. In addition, a one-way ANOVA test indicated that there were no statistical differences between the four groups using a significance threshold of 0.05 (95%; see Appendix).

$\delta^{18}\text{O}_{\text{sw}}$ (VSMOW) values were calculated from carbonate $\delta^{18}\text{O}$ (VPDB) and $T(\Delta_{47})$ following Kim and O'Neil (1997) (Table 3). Calculated $\delta^{18}\text{O}_{\text{sw}}$ values ranged from -4.9 to 4.9‰ (VSMOW). Below 50cm depth, $\delta^{18}\text{O}_{\text{sw}}$ values for CAN01, CAN02, and DL01 were similar, ranging between 0.3 and 2.6‰. Nacuñan values below 50cm depth were more negative, ranging between -4.9 and -3.5‰.

Table 3: Summary of isotopic analyses for carbonate samples

Sample:	<i>n</i>	$\delta^{13}\text{C}^{\text{a}}$ (‰) (VPDB)	$\delta^{18}\text{O}^{\text{a}}$ (‰) (VPDB)	$\Delta_{47} \pm 1\text{SE}^{\text{a}}$ (‰)	$T(\Delta_{47}) \pm 1\text{SE}$ (°C)			Soil water $\delta^{18}\text{O}^{\text{b}}$ (‰) (VSMOW)		
				Calibration:	Zaarur et al., 2013	Dennis et al., 2011	Ghosh et al., 2006	Zaarur et al., 2013	Dennis et al., 2011	Ghosh et al., 2006
CAN01, 1.0km elevation										
10cm	3	-1.84	-3.7	$0.638 \pm 0.011^{\text{c}}$	42 ± 3	50 ± 5		1.9 ± 0.6	3.4 ± 1.9	
25cm	3	-0.29	-2.2	$0.676 \pm 0.011^{\text{c}}$	32 ± 3	34 ± 4		1.4 ± 0.7	1.9 ± 1.9	
40cm	3	-1.89	-3.4	0.666 ± 0.016	34 ± 4	38 ± 7		0.7 ± 0.8	1.4 ± 2.6	
55cm	3	-3.13	-3.4	0.674 ± 0.016	32 ± 4	35 ± 6		0.3 ± 0.8	0.8 ± 2.5	
70cm	2	-3.47	-1.9	0.660 ± 0.018	36 ± 5	41 ± 8		2.6 ± 1.0	3.6 ± 3.0	
100cm	2	-2.63	-3.2	0.677 ± 0.045	31 ± 11	33 ± 18		0.4 ± 3.5	0.9 ± 8.4	
Pit average:		-3.08	-2.8	0.670 ± 0.026	34 ± 5	38 ± 8		$1.1 \pm 1.8^*$	$1.7 \pm 4.6^*$	
CAN02, 1.0km elevation										
10cm	3 ^d	-0.95	0.9	$0.676 \pm 0.011^{\text{c}}$	32 ± 3	34 ± 4		4.6 ± 0.5	5.1 ± 1.7	
25cm	3 ^d	-3.11	2.3	0.698 ± 0.014	26 ± 3	25 ± 5		4.9 ± 0.7	4.8 ± 2.1	
40cm	2 ^d	-3.75	0.8	$0.680 \pm 0.013^{\text{c}}$	30 ± 3	32 ± 5		4.3 ± 0.6	4.6 ± 2.1	
55cm	2 ^d	-4.66	-0.1	0.685 ± 0.030	29 ± 7	30 ± 12		3.1 ± 1.4	3.3 ± 4.7	
70cm	3 ^d	-2.08	-0.8	0.693 ± 0.017	27 ± 4	27 ± 6		2.1 ± 0.8	2.1 ± 2.7	
85cm	3 ^d	-3.86	-1.9	0.706 ± 0.013	24 ± 3	22 ± 5		0.3 ± 0.6	0.0 ± 2.0	
100cm	2 ^d	-5.01	-1.8	0.683 ± 0.030	30 ± 8	31 ± 12		1.6 ± 1.4	1.8 ± 4.7	
Pit average:		-3.90	-1.1	0.692 ± 0.023	28 ± 5	29 ± 7		$1.8 \pm 1.1^*$	$1.8 \pm 3.5^*$	
CAN03, 1.0km elevation										
50cm	3	-4.66	-2.9	$0.679 \pm 0.011^{\text{c}}$	31 ± 3	33 ± 4		0.6 ± 0.6	1.0 ± 1.8	
DL01, 1.0km elevation										
20cm	3	-1.19	-1.0	$0.650 \pm 0.011^{\text{c}}$	38 ± 3	45 ± 5		3.9 ± 0.5	5.1 ± 1.8	
40cm	4	-4.11	-1.4	0.698 ± 0.020	26 ± 5	25 ± 7		1.2 ± 1.0	1.1 ± 3.1	
70cm	2	-5.21	-2.5	$0.685 \pm 0.013^{\text{c}}$	29 ± 3	30 ± 5		0.7 ± 0.7	0.9 ± 2.1	
100cm	2	-5.18	-3.0	$0.655 \pm 0.013^{\text{c}}$	37 ± 4	43 ± 6		1.7 ± 1.1	2.8 ± 2.6	
Pit average:		-5.19	-2.8	0.670 ± 0.011	33 ± 4	36 ± 6		$1.2 \pm 0.9^*$	$1.9 \pm 2.4^*$	
Nacuñan, 0.6km elevation *(carbonate nodule samples)										
20cm	3	-5.54	-6.7	0.703 ± 0.014	25 ± 3	24 ± 5		-4.4 ± 0.8	-4.6 ± 2.2	
50cm	4 ^d	-6.01	-8.3	0.652 ± 0.013	38 ± 4	44 ± 6		-3.5 ± 0.7	-2.3 ± 2.2	
85cm	3 ^d	-5.67	-7.6	$0.695 \pm 0.011^{\text{c}}$	27 ± 3	26 ± 4		-4.8 ± 0.5	-4.9 ± 1.7	
100cm	2	-5.53	-8.5	$0.678 \pm 0.013^{\text{c}}$	31 ± 3	33 ± 5		-4.9 ± 0.9	-4.5 ± 2.4	
Pit average:		-5.60	-8.0	0.686 ± 0.012	30 ± 3	35 ± 5		$-4.4 \pm 0.7^*$	$-3.9 \pm 2.1^*$	
Peters et al. 2013, 1.1km elevation										
Pit average:		-5.11^e	-2.7^e	$0.671 \pm 0.023^{\text{c}}$			20 ± 4			-1.4 ± 0.7
Peters et al. 2013, 1.6km elevation										
Pit average:		-5.99^e	-10.5^e	$0.675 \pm 0.013^{\text{c}}$			19 ± 3			-9.4 ± 0.6

^a Carbonate $\delta^{13}\text{C}$, $\delta^{18}\text{O}$, reported as mean and Δ_{47} reported as weighted mean of replicates (*n*) for each individual sample. Average external error (1SE) for replicates of a sample is $\pm 0.03\text{‰}$ for $\delta^{13}\text{C}$, $\pm 0.028\text{‰}$ for $\delta^{18}\text{O}$, and $\pm 0.019\text{‰}$ for Δ_{47} .

^b Soil water $\delta^{18}\text{O}$ was calculated using the calcite-water O-isotope fractionation equation of Kim and O'Neil (1997). Uncertainty in soil water $\delta^{18}\text{O}$ was calculated by propagating errors in $T(\Delta_{47})$. *Soil pit averages for $\delta^{18}\text{O}_{\text{sw}}$ were calculated for samples of depth >50cm.

^c For samples with low SE for replicates, SE was assigned using the long-term SD of a standard run during the same period of time divided by \sqrt{n} , where *n* is the number of sample replicates, following Peters et al. (2013) and Huntington et al. (2009).

^d Samples noted with *n*^d were analyzed using an additional two replicates for $\delta^{13}\text{C}$ and $\delta^{18}\text{O}$ measurements using a Kiel III Carbonate Device coupled to a dual-inlet Thermo Finnigan Delta Plus IRMS at the University of Washington Isolab.

^e Peters et al., (2013) (pre-ARF) average external error (1SE) for replicates is $\pm 0.04\text{‰}$ for $\delta^{13}\text{C}$, $\pm 0.002\text{‰}$ for $\delta^{18}\text{O}$, and $\pm 0.016\text{‰}$ for Δ_{47} . Replicates in ARF for 50 cm samples at 1.1 and 1.6 km yielded $T(\Delta_{47})$ values differing from original publication by < 2°C

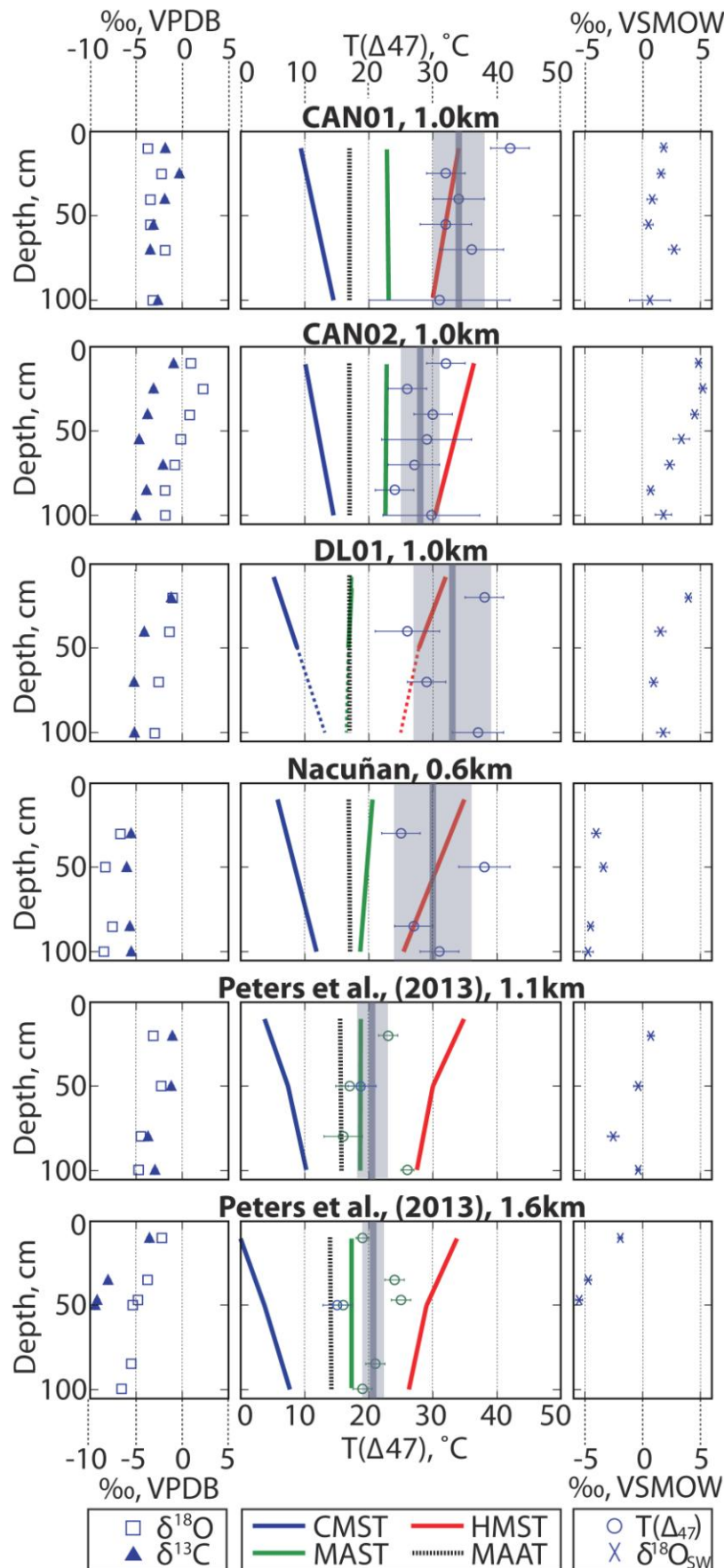


Figure 5: Soil carbonate isotope data for CAN01, CAN02, DL01, and Nacuñan (this study), followed by 1.1km and 1.6km data from nearby E-W Río Mendoza valley elevation transect study (Peters et al.2013)

Left panels: carbonate $\delta^{13}\text{C}$ VPDB (triangles) and carbonate $\delta^{18}\text{O}$ VPDB (squares)

Middle panels: soil carbonate $T(\Delta_{47}) \pm 1\text{SE}$ following Zaarur et al. (2013) (circles). Gray vertical bars and shaded boxes indicate the mean and standard deviation across all $T(\Delta_{47})$ in a soil profile. Lines represent coldest mean soil temperature (CMST, blue), mean annual soil temperature (MAST, green), hottest mean soil temperature (HMST, red), and mean annual air temperature (MAAT, black), extrapolated from 1 year of soil temperatures recorded by sensors at 10, 50, and 100cm, from air temperatures recorded at Mendoza Airport (CAN01, CAN02, DL01), and by instrumentation at Nacuñan.

[Note: Peters $T(\Delta_{47})$ data were calculated using the Ghosh et al. (2006) calibration and were not reported in the absolute reference frame, with the exception of replicated 50 cm samples.]

Right panels: calculated $\delta^{18}\text{O}$ of soil water (VSMOW) (crosses).

4.3 Carbonate saturation modeling results

Soil temperature and pCO₂ sensor data for the Nacuñan site were used to calculate the activity of calcite as described in Equation 3, assuming that carbonate formation is an equilibrium process (Figure 4). Soil solution Ca²⁺ concentration is assumed at a constant near-saturation value of 1.5 mmol/L (Rossi and Villagra, 2003). Temperature-dependent equilibrium constants K₁, K₂, K_{cal}, and K_{CO2} were calculated using parameters from Plummer and Busenberg (1982). Calcite activities calculated for Nacuñan for the period February 2014 and May 2014 were always greater than 1, suggesting persistent conditions of CaCO₃ supersaturation throughout the year (Figure 4). The lowest activity values ($\alpha = 1.7$) occurred in early March 2014, coincident with the maximum observed soil pCO₂.

5. Discussion

5.1 Potential for variability in $T(\Delta_{47})$ between sites

In all soil pits, $\delta^{13}\text{C}$ and $\delta^{18}\text{O}$ values generally increase towards the surface. We interpret this to be indicative of undisturbed soil profiles with soil water evaporation near the surface and soil gas exchange with atmospheric CO₂, respectively (Cerling and Quade, 1993). Below 50 cm depth, the range of $\delta^{13}\text{C}$ values (-5.0‰ to -2.1‰) at CAN01 and CAN02 reflects a lower soil productivity and potentially higher C₄/C₃ distribution than at DL01 and Nacuñan (-6.0‰ to -5.2‰) (Cerling, 1988).

$T(\Delta_{47})$ values averaged over depth for the CAN01, CAN02, DL01, and Nacuñan soil profiles are not significantly different. This suggests that sites chosen in a single precipitation regime at a single elevation will be indistinguishable in $T(\Delta_{47})$ even under varying C₃/C₄ distributions. This challenges the expectation that soil carbonate formation temperatures will be

higher under C₄ plant growth (most productive in summer) than under C₃ plant growth (adapted to cooler conditions) (Breecker et al. 2009; Meyer et al. 2014).

While our $T(\Delta_{47})$ values are statistically indistinguishable between 4 nearby sites in this study, our $T(\Delta_{47})$ values exceed those of the nearest 2 Peters et al. (2013) sites by $\sim 10^\circ\text{C}$, despite surface and *in-situ* conditions that are comparable. This suggests that there is a potential for substantial variability in $T(\Delta_{47})$ at the same elevation in a region dominated by the same precipitation and vegetation regime. The nearest Peters site (1.1 km) differs from DL01 by only 100 m elevation and 20 km distance; it may be possible that local topographic features, or a difference in soil temperature or water chemistry may contribute to a difference in carbonate formation and associated $T(\Delta_{47})$ values. In particular, the Peters 1.1km site lies <0.5 km from the Mendoza River, which may have been subject to periodic flooding that could alter soil moisture and chemistry in this site. Further investigation into the sub-surface physical and chemical differences between these sites will be necessary to say more about the potential impacts on $T(\Delta_{47})$ values.

5.2 Invariance of $T(\Delta_{47})$ with depth

$T(\Delta_{47})$ values within each sampled pit were found to vary little with depth (Figure 5, middle panels), consistent with other studies (Quade et al., 2013; Peters et al., 2013). The simplest explanation for this invariance would be carbonate formation during the spring or fall when the soil profile is near isothermal, such that range of $T(\Delta_{47})$ values would be constrained through the soil profile. Our instrumental temperature records show that the conditions for a seasonally isothermal soil occur over a narrow range of time (1-2 weeks) during the spring and fall in which soil temperatures are near MAAT. However, our observed $T(\Delta_{47})$ values range

from 28 to 34°C and are at least 10°C higher than spring or fall temperatures at any instrumented soil pit, suggesting that some other process must account for the observed temperature invariance with depth.

5.3 Isothermal conditions after rainfall events

In all 4 sites, soil moisture sensors installed at 50cm captured one significant soil wetting event in late February, immediately after which near-isothermal conditions were registered at 10, 50, and 100cm (Figure 6, top panel). At CAN01, soil temperatures converge at ~30°C over 1-2 days, at the low range of $T(\Delta_{47})$ for this site (Figure 6). If carbonate were to form at this time at any depth in the soil, its $T(\Delta_{47})$ would contribute to a hot, isothermal $T(\Delta_{47})$ soil profile, such as we see in Figure 5. These near-isothermal conditions persist for ~1-3 days after the precipitation event, and though the soil is only just beginning to dry, our calculations of aqueous calcite activity suggest that conditions of high Ca^{2+} and low CO_2 at this time will result in a soil solution that is supersaturated in CaCO_3 . During the months after this event in which the soil dries back to dry baseline conditions, soil temperatures fall well below the range of $T(\Delta_{47})$ values for this site.

Observed soil temperatures were several degrees higher at the peak of summer for CAN02 than for CAN01, and soil conditions at CAN02 at 50cm depth were dry throughout the recorded year. However, some wetting was observed at the same late February event, and sensors registered a significant drop in soil temperature resulting in near-isothermal conditions at ~30°C, roughly agreeing with the average $T(\Delta_{47})$ value calculated for this site.

While the DL01 site was located only ~40km away from the CAN01 and CAN02 sites, it experienced much wetter conditions between August 2013 and August 2014. Immediately after

wetting events in late November and late February (summer), soil temperature sensors at 10 and 50cm registered isothermal conditions at $\sim 25\text{-}27^{\circ}\text{C}$, falling just at or below the lower range of average $T(\Delta_{47})$ value calculated for this site. Soil temperatures recorded after an April 2014 (fall) wetting event never reached isothermal conditions.

One significant soil wetting event was registered for Nacuñan at 50cm depth in late February 2014, with precipitation infiltrating through to the 100 cm depth soil moisture sensor. Soil temperatures at this site converged at $\sim 27^{\circ}\text{C}$ immediately after this event, within the calculated $T(\Delta_{47})$ range.

One minor soil wetting event was registered in January 2011(summer) at the 1.1 km Peters site, in which soil moisture levels remained below $0.10\text{m}^3/\text{m}^3$ (dry), while soil temperatures decreased to isothermal conditions at $\sim 23^{\circ}\text{C}$, matching $T(\Delta_{47})$ for this site.

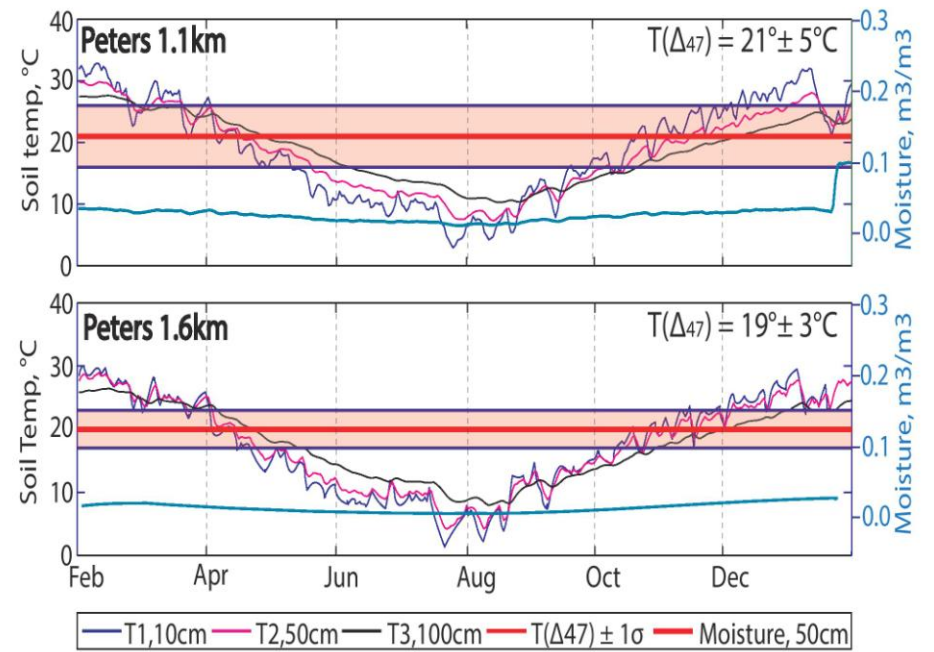
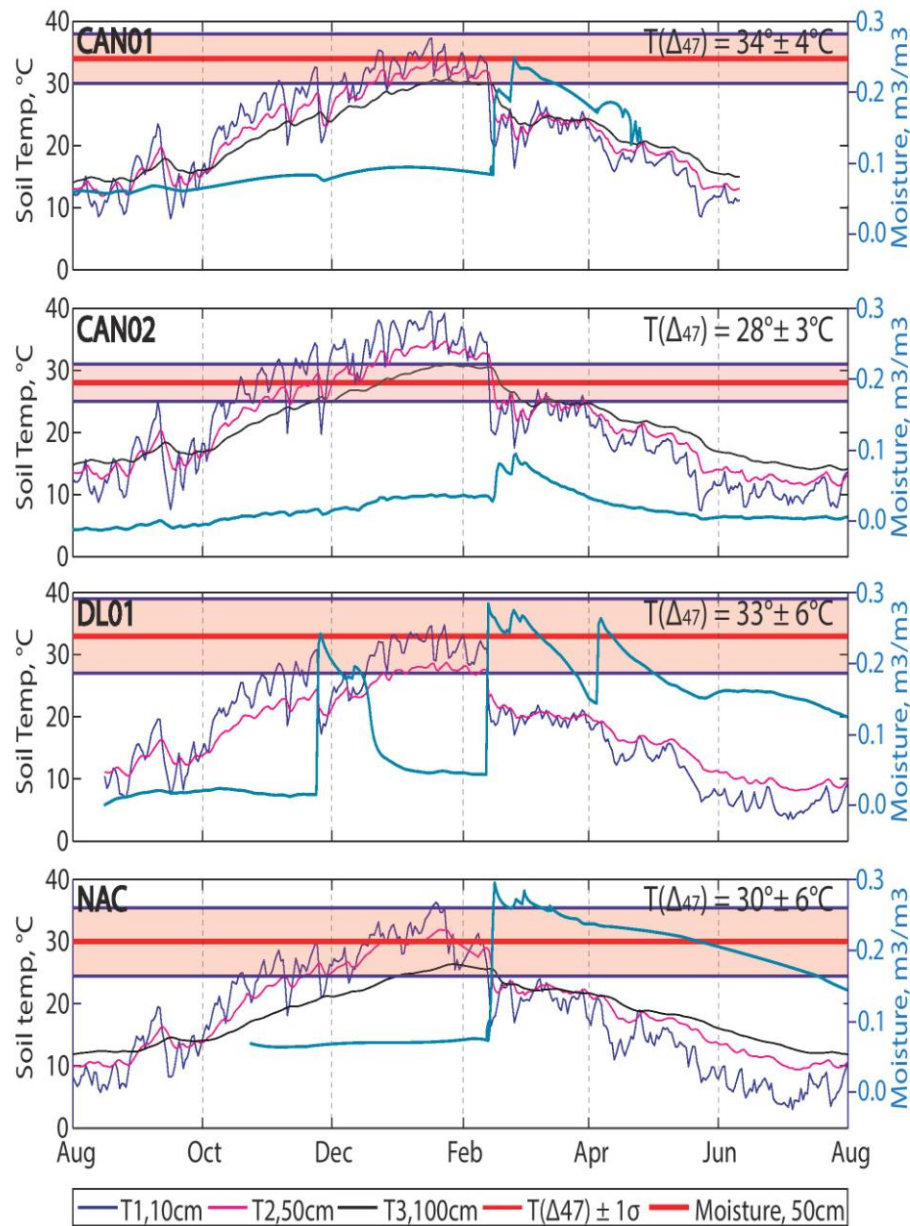


Figure 6: Isothermal conditions immediately after large wetting events at 50cm depth for 4 instrumented sites, August 2013-August 2014 (*this study*); nearest 2 Peters sites, February 2010-January 2011 (*Peters et al. 2013*)

Generally, *in-situ* soil temperatures recorded at all four sites immediately following significant soil wetting events are similar to carbonate formation clumped isotope temperatures and reflect the isothermal conditions seen in our clumped isotope $T(\Delta_{47})$ profiles. CAN02 and Nacuñan are the best examples of this, where soil temperatures after wetting events are isothermal and match calculated $T(\Delta_{47})$, while soil temperatures for CAN01 and DL01 fall at or slightly below their $T(\Delta_{47})$ ranges.

Our findings are consistent with a recent study using carbonates from Wyoming and Nebraska by Hough et al. (2014), who argued that soil carbonate forms during early summer soil drying and drying after mid-late summer rainfall events. By providing soil temperature and moisture data with depth, we build on Hough et al. (2014) to suggest that high temperatures and isothermal conditions recorded in Δ_{47} signals are accounted for by carbonate formation occurring immediately after large precipitation events during the hottest months of summer, and not during the progressive drying out of the soil on the tail end of the wet season as suggested by Breecker et al. (2009). This further constrains the window of carbonate formation to brief events when the soil is just beginning to dry out, rather than during the several weeks of drying necessary to return soil moisture to its baseline condition at 50 cm depth.

5.4 Seasonal controls on soil carbonate $T(\Delta_{47})$

We use equation 2 as a simple equilibrium-based first-pass model for determining the seasonality of carbonate supersaturation in soil, although disequilibrium fractionation cannot be completely discounted. Calcite activity calculations for Nacuñan indicate constant carbonate supersaturation that should allow for calcite precipitation at any time that water is removed from the soil (Figure 4). As plant activity dies down in winter and the soil dries out, activities rise,

indicating increasing calcite supersaturation. $p\text{CO}_2$ is a major control on calcite saturation, such that activities only approach 1 during midsummer, when $p\text{CO}_2$ increases rapidly in response to large rainstorms. Surface soils in this region have relatively high Ca^{2+} concentration of 1.5-2.0 mmol/L and should be near-constant with depth (Jobbagy and Jackson 2001; Rossi and Villagra 2003). In order to arrive at conditions that favor calcite dissolution, ($\alpha_{\text{calcite}} < 1$), Ca^{2+} concentrations must fall below 1.2 mmol/L in March - May 2014 when $p\text{CO}_2$ is highest, below 1.0 mmol/L for May 2014 - September 2014, and below 0.75 mmol/L for September 2014 onwards, when $p\text{CO}_2$ continues to decrease. In these well-drained arid soils, it is reasonable to expect high Ca^{2+} concentrations throughout the soil profile, such that calcite supersaturation is maintained throughout the year. Further field data on Ca^{2+} concentrations in soil water would be necessary to continue this line of inquiry, but for the period of data available, we expect that calcium carbonate is potentially able to form at any time of the year. Since soil carbonates represent formation integrated over a period of hundreds to thousands of years, carbonate formation must be far more frequent under summer conditions, in our case the wet season, than throughout the rest of the year, based on $T(\Delta_{47})$ and *in-situ* temperatures. However, the lowest Peters et al. (2013) sites, subject to identical field conditions, do not seem to agree with our observations in the piedmont. Potential differences include a difference in the soil water chemistry or soil moisture, since the Mendoza River transports limestone rich sediment from the high Andes and may have been subject to periodic flooding.

In the context of soil wetting events discussed above, the supersaturated conditions inferred from calcite activity, combined with the isothermal soil conditions observed immediately following the largest rainfall events, suggest that calcium carbonate forms seasonally in relation to these large wetting events. While soil solution conditions are likely to be

supersaturated throughout the rest of the year, *in-situ* conditions are so dry that without some change in soil moisture conditions we should not expect any significant carbonate formation. The seasonality of rainfall in this region should therefore result in a carbonate clumped T(Δ_{47}) record biased towards summer soil temperatures, consistent with our observations.

5.5 Implications for isotopic records from pedogenic carbonates

This study results in 3 key findings that should inform future application of the clumped isotope geothermometer to estimate formation temperatures of pedogenic carbonates.

- 1) For arid to semi-arid field sites under the same precipitation regime and at similar elevations (0.6km to 1.0km), site-to-site variability in soil carbonate (clast coating or nodule) T(Δ_{47}) records are likely to be negligible. This is important for applications of the clumped isotope geothermometer in paleoaltimetry or paleoenvironmental studies; if a site is known to have predominantly C₃ or C₄ plant types, pedogenic clumped isotope T(Δ_{47}) records need not be adjusted to account for vegetation type. However, there is significant variation between T(Δ_{47}) values calculated for this study and for values from very similar nearby sites (Peters et al., 2013). This suggests the potential for strong local controls that may result in spatial variability in soil carbonate T(Δ_{47}), though no variation was seen between CAN01, CAN02, DL01, and Nacuñan sites in this study.
- 2) Similar to previous studies, T(Δ_{47}) values for CAN01, CAN02, DL01, and Nacuñan sites were found to be invariant to 1m depth suggesting that soil carbonate formation is restricted to intervals when the soil profile is isothermal, which occurs during either the transition in seasons or after large summer rainstorms, or that some other process drives carbonate formation such that hot, summer T(Δ_{47}) values are recorded without variation with depth.

- 3) Under a summer-only precipitation regime in a semi-arid region, $T(\Delta_{47})$ values reflect the isothermal summer soil temperatures that occur just after large rainfall events that result in significant soil wetting. Thus, potential (paleo)precipitation regimes should be carefully considered when applying the carbonate clumped isotope geothermometer to paleoenvironmental reconstructions.

5.6 Recommendations for future work

- 1) Continued *in-situ* data collection, particularly for soil CO₂ data, during years with more typical mean annual precipitation, would allow for comparison of $T(\Delta_{47})$ values with *in-situ* data that better represent long-term conditions in this region. Collection of soil water chemistry data, particularly for soil solution Ca²⁺, at all 4 sites and at the Peters 1.1 km site would provide a better basis for investigation of calcite activities and for comparison of chemical factors that might result in a 10⁰C temperature shift between the CAN/DL sites and Peters.
- 2) This study focused on pure C₃ and ~50/50 C₃/C₄ environments. Carbonate collection and analysis from soil profiles within a pure C₄ environment (i.e., grasslands) would allow for a better comparison of $T(\Delta_{47})$ records under varying plant types.
- 3) Monitored, in-laboratory carbonate growth experiments under controlled conditions that simulate arid soils would provide a better test of the timing of carbonate precipitation than our use of a simple equilibrium model.

6. Conclusions

With its summer-only precipitation regime and C₃/C₄ transition, the eastern Andean Piedmont is an ideal location for investigating the variation in pedogenic carbonates clumped isotope records. In this region at an elevation of ~0.6-1.0km, we find that carbonate clumped isotope temperatures are invariant between sites of ~ 0.02 - 0.46 C₄/total vegetation biomass by groundcover. Carbonate formation temperatures fall at or above the hottest mean monthly soil temperatures and are isothermal between 10cm and 100cm depth. T(Δ₄₇) values coincide with *in-situ* soil temperatures measured immediately after significant summer rainfall events. We suggest that the timing of carbonate formation in arid regions with a summer precipitation regime is driven by seasonal rainfall, where isothermal summer soil temperatures are captured immediately after large rainfall events that result in significant soil wetting.

Appendix A: In situ site data

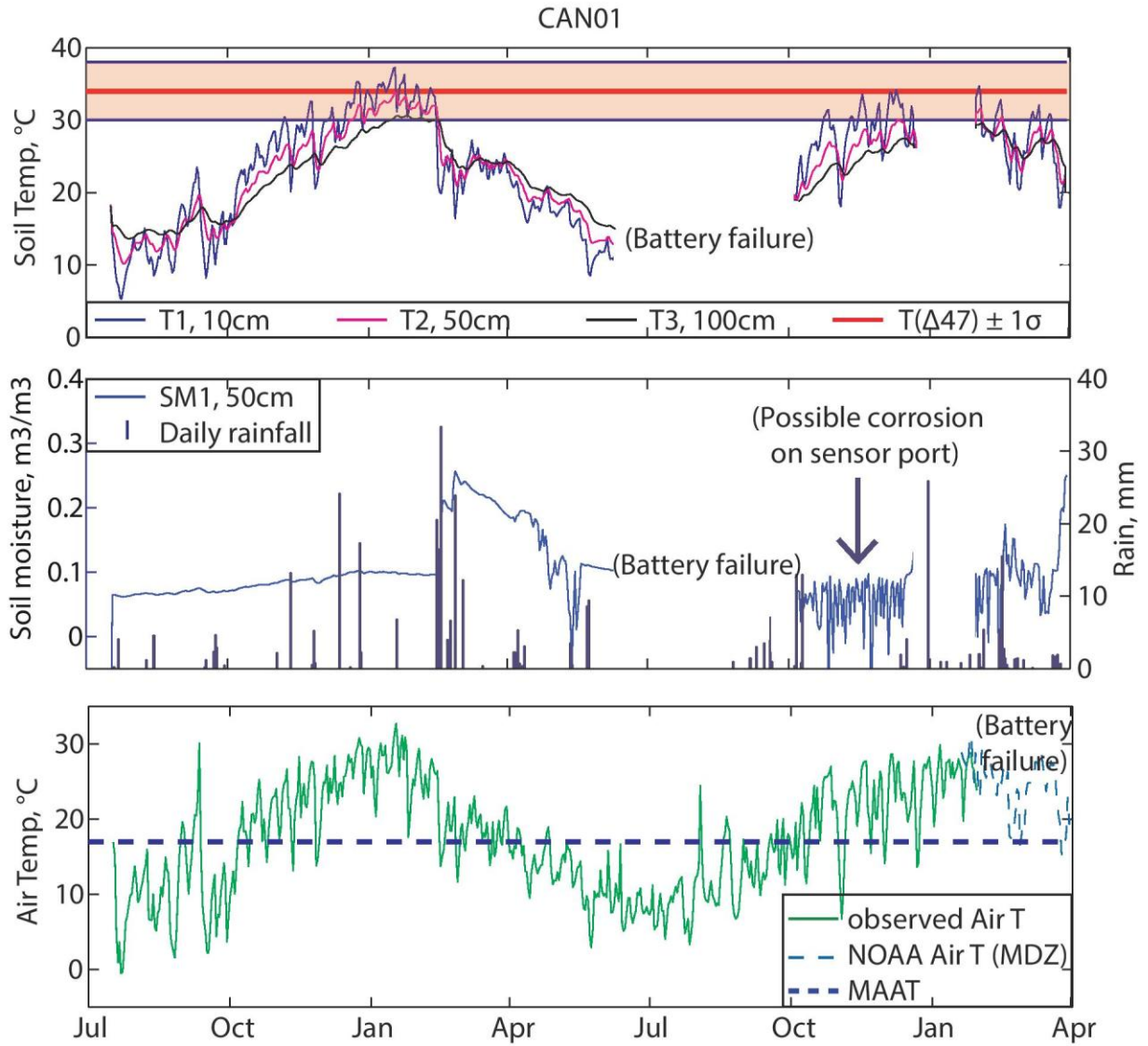


Figure A1: CAN01 sensor data averaged daily: Soil temperatures (*top*), soil moisture (*bottom*), and air temperature sensor data (*bottom*) for the months of July 2013-March 2015. Precipitation data are averaged between BDHI and NOAA records from Mendoza, Argentina. Missing data beginning in July 2014 and again in January 2015 is due to dead batteries. Soil moisture sensor misbehavior in the months May 2014 and October 2014 may be due to water in the micrologger case or a damaged soil moisture sensor cable.

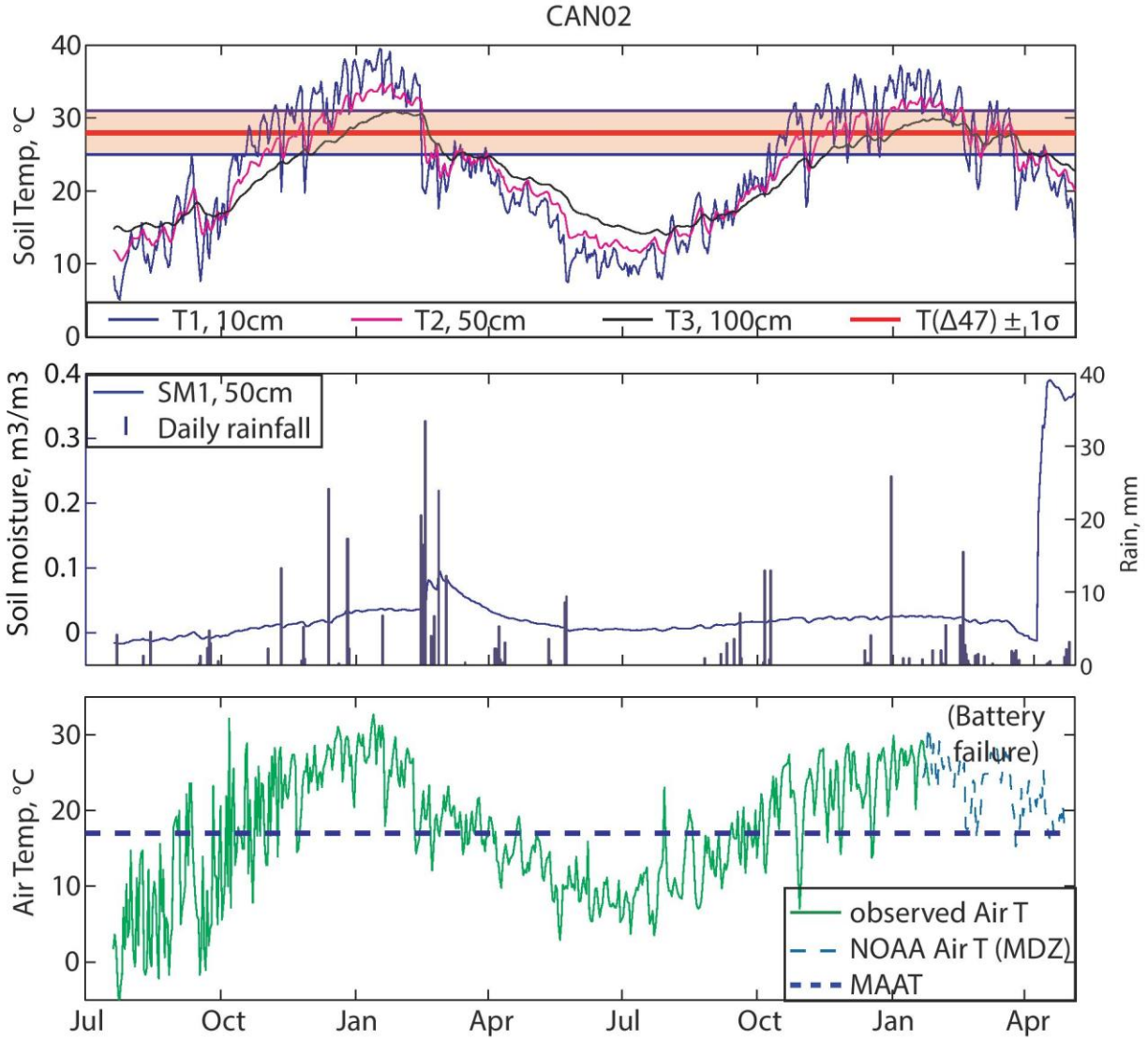


Figure A2: CAN02 sensor data averaged daily: Soil temperatures (*top*), soil moisture (*bottom*), and air temperature sensor data (*bottom*) for the months of July 2013-May 2015. Precipitation data are averaged between BDHI and NOAA records from Mendoza, Argentina. Due to a sensor malfunction, air temperature data between July 2013 and November 2013 is taken from NOAA records from Mendoza, Argentina, after which point the pendant logger for air temperature was replaced.

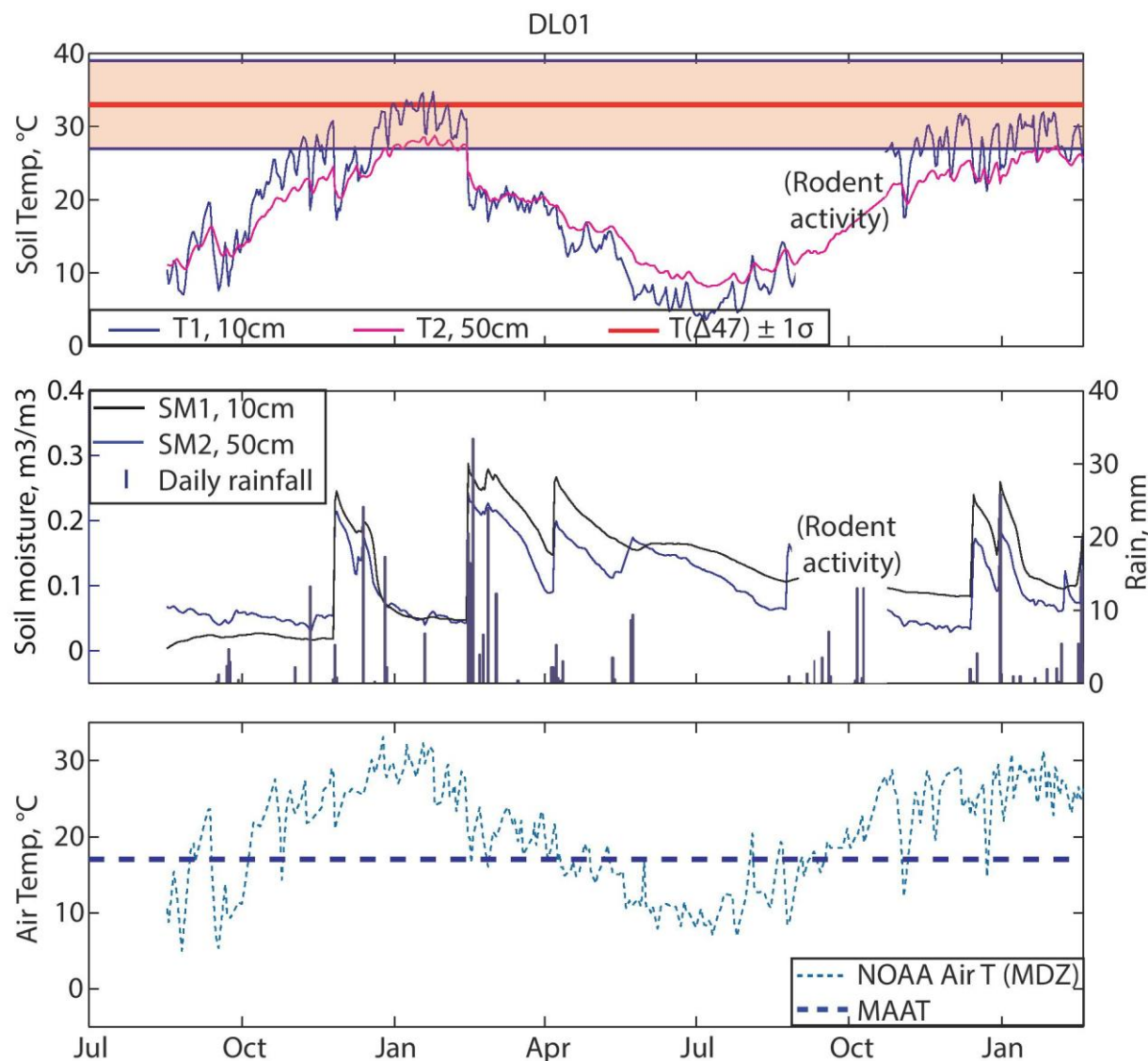


Figure A3: DL01 sensor data averaged daily: Soil temperatures (*top*), soil moisture (*bottom*), and air temperature sensor data (*bottom*) for the months of August 2013-February 2015. Precipitation data are averaged between BDHI and NOAA records from Mendoza, Argentina. Air temperature data are taken from NOAA records from Mendoza, Argentina. Missing data during the months of September through October 2014 is due to severed cables by rodent activity.

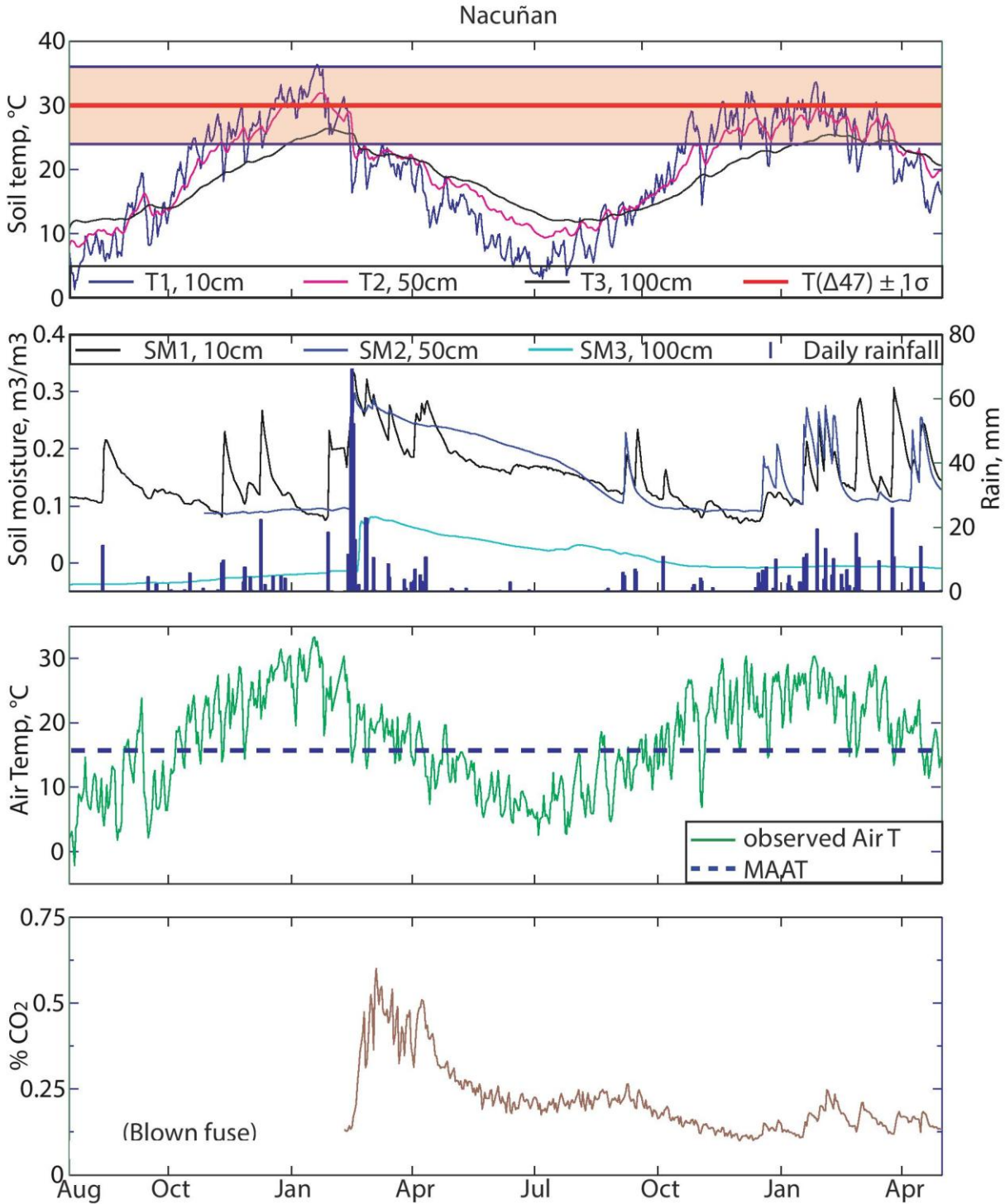


Figure A4: Nacuñan sensor data: Soil temperatures, soil moisture, air temperature, and soil CO₂ sensor data for the months of July 2013-May 2015. Soil CO₂ data are missing before February 2014 due to a blown fuse in the power system.

Appendix B: Summary of all isotopic analyses

Table B1: Summary for all replicates of isotopic analyses for carbonate samples

Sample (Replicate #)	Elevation (m)	Depth (cm)	Latitude (S)	Longitude (W)	$\delta^{13}\text{C}^a$ (‰, VPDB)	$\delta^{18}\text{O}^a$ (‰, VPDB)	$\Delta_{47} \pm 1\text{SE}^a$ (‰)	$T(\Delta_{47}) \pm 1\text{SE}$ (°C)	Soil water $\delta^{18}\text{O}^b$ (‰, VSMOW)
CAN01-10	1000	10	32° 35' 31.44''S	68° 54' 19.26''W	-1.84	-3.7	0.638 ± 0.011^c	42 ± 3	1.9 ± 0.6
(1)					-1.92	-3.5	0.634 ± 0.009		
(2)					-1.83	-3.8	0.634 ± 0.007		
(3)					-1.78	-3.8	0.646 ± 0.007		
CAN01-25	1000	25	32° 35' 31.44''S	68° 54' 19.26''W	-0.29	-2.2	0.676 ± 0.011^c	32 ± 3	1.4 ± 0.7
(1)					-0.36	-2.4	0.679 ± 0.007		
(2)					-0.26	-2.0	0.691 ± 0.008		
(3)					-0.26	-2.4	0.658 ± 0.008		
CAN01-40	1000	40	32° 35' 31.44''S	68° 54' 19.26''W	-1.89	-3.4	0.666 ± 0.016	34 ± 4	0.7 ± 0.8
(1)					-1.94	-3.4	0.682 ± 0.009		
(2)					-1.87	-3.4	0.635 ± 0.009		
(3)					-1.86	-3.6	0.683 ± 0.008		
CAN01-55	1000	55	32° 35' 31.44''S	68° 54' 19.26''W	-3.13	-3.4	0.674 ± 0.016	32 ± 4	0.3 ± 0.8
(1)					-3.15	-3.5	0.704 ± 0.008		
(2)					-3.13	-3.3	0.649 ± 0.008		
(3)					-3.11	-3.4	0.670 ± 0.008		
(4) ^d					-3.08	-3.6	1.882 ± 0.008		
CAN01-70	1000	70	32° 35' 31.44''S	68° 54' 19.26''W	-3.47	-1.9	0.660 ± 0.018	36 ± 5	2.6 ± 1.0
(1)					-3.46	-1.7	0.678 ± 0.008		
(2)					-3.47	-2.0	0.642 ± 0.009		
CAN01-100	1000	100	32° 35' 31.44''S	68° 54' 19.26''W	-2.63	-3.2	0.677 ± 0.045	31 ± 11	0.4 ± 3.5
(1)					-2.58	-4.6	0.722 ± 0.009		
(2)					-2.67	-1.7	0.633 ± 0.009		
CAN02-10	1000	10	32° 39' 07.46''S	68° 55' 0.10''W	-0.95	0.9	0.676 ± 0.011^c	32 ± 3	4.6 ± 0.5
(1)					-2.73	-1.6	0.681 ± 0.008		
(2)					-0.53	1.5	0.677 ± 0.009		
(3)					-0.48	1.5	0.669 ± 0.008		
(Kiel (1))					-0.36	1.5			
(Kiel (2))					-0.67	1.9			
CAN02-25	1000	25	32° 39' 07.46''S	68° 55' 0.10''W	-3.11	2.3	0.698 ± 0.014	26 ± 3	4.9 ± 0.7
(1)					-0.60	1.6	0.678 ± 0.009		
(2)					-3.75	2.3	0.692 ± 0.009		
(3)					-3.74	2.1	0.725 ± 0.010		
(Kiel (1))					-3.75	2.6			
(Kiel (2))					-3.69	2.8			

Sample (Replicate #)	Elevation (m)	Depth (cm)	Latitude (S)	Longitude (W)	$\delta^{13}\text{C}^a$ (‰, VPDB)	$\delta^{18}\text{O}^a$ (‰, VPDB)	$\Delta_{47} \pm 1\text{SE}^a$ (‰)	$T(\Delta_{47}) \pm 1\text{SE}$ (°C)	Soil water $\delta^{18}\text{O}^b$ (‰, VSMOW)
CAN02-40	1000	40	32° 39' 07.46''S	68° 55' 0.10''W	-3.75	0.8	0.680 ± 0.013^c	30 ± 3	4.3 ± 0.6
(1)					-3.72	2.6	0.688 ± 0.008		
(2)					-3.73	-0.0	0.672 ± 0.009		
(Kiel (1))					-3.92	0.3			
(Kiel (2))					-3.62	0.3			
CAN02-55	1000	55	32° 39' 07.46''S	68° 55' 0.10''W	-4.66	-0.1	0.685 ± 0.030	29 ± 7	3.1 ± 1.4
(1)					-4.52	-0.7	0.715 ± 0.009		
(2)					-4.71	-0.4	0.655 ± 0.008		
(Kiel (1))					-4.72	0.1			
(Kiel (2))					-4.70	0.4			
CAN02-70	1000	70	32° 39' 07.46''S	68° 55' 0.10''W	-2.08	-0.8	0.693 ± 0.017	27 ± 4	2.1 ± 0.8
(1)					-4.01	0.3	0.660 ± 0.011		
(2)					-1.57	-1.6	0.719 ± 0.007		
(3)					-1.63	-1.4	0.698 ± 0.009		
(Kiel (1))					-1.49	-0.8			
(Kiel (2))					-1.72	-0.4			
CAN02-85	1000	85	32° 39' 07.46''S	68° 55' 0.10''W	-3.86	-1.9	0.706 ± 0.013	24 ± 3	0.3 ± 0.6
(1)					-1.60	-1.2	0.700 ± 0.010		
(2)					-4.40	-2.3	0.732 ± 0.011		
(3)					-4.46	-2.2	0.687 ± 0.009		
(Kiel (1))					-4.36	-2.0			
(Kiel (2))					-4.48	-1.6			
CAN02-100	1000	100	32° 39' 07.46''S	68° 55' 0.10''W	-5.01	-1.8	0.683 ± 0.030	30 ± 8	1.6 ± 1.4
(1)					-4.25	-1.8	0.653 ± 0.020		
(2)					-5.16	-2.1	0.713 ± 0.009		
(Kiel (1))					-5.46	-1.7			
(Kiel (2))					-5.18	-1.5			
CAN03-50	1000	50	32° 34' 12.28''S	68° 56' 33.68''W	-4.66	-2.9	0.679 ± 0.011^c	31 ± 3	0.6 ± 0.6
(1)					-4.64	-3.1	0.667 ± 0.009		
(2)					-4.62	-3.0	0.686 ± 0.008		
(3)					-4.72	-2.7	0.683 ± 0.008		
DL01-20	1000	20	32° 52' 40.22''S	68° 55' 20.98''W	-1.19	-1.0	0.650 ± 0.011^c	38 ± 3	3.9 ± 0.5
(1)					-1.20	-1.0	0.656 ± 0.008		
(2)					-1.21	-1.1	0.664 ± 0.007		
(3)					-1.15	-1.0	0.631 ± 0.008		
DL01-40	1000	40	32° 52' 40.22''S	68° 55' 20.98''W	-4.11	-1.4	0.698 ± 0.020	26 ± 5	1.2 ± 1.0
(1)					-4.13	-1.4	0.757 ± 0.006		
(2)					-4.13	-1.2	0.669 ± 0.006		
(3)					-4.09	-1.5	0.686 ± 0.007		
(4)					-4.10	-1.4	0.681 ± 0.008		

Sample (Replicate #)	Elevation (m)	Depth (cm)	Latitude (S)	Longitude (W)	$\delta^{13}\text{C}^a$ (‰, VPDB)	$\delta^{18}\text{O}^a$ (‰, VPDB)	$\Delta_{47} \pm 1\text{SE}^a$ (‰)	$T(\Delta_{47}) \pm 1\text{SE}$ (°C)	Soil water $\delta^{18}\text{O}^b$ (‰, VSMOW)
<i>DL01-70</i> (1)	<i>1000</i>	<i>70</i>	<i>32° 52' 40.22''S</i>	<i>68° 55' 20.98''W</i>	<i>-5.21</i>	<i>-2.5</i>	<i>0.685 ± 0.013^c</i>	<i>29 ± 3</i>	<i>0.7 ± 0.7</i>
(2)					-5.21	-2.597	0.689 ± 0.007		
<i>DL01-100</i> (1)	<i>1000</i>	<i>100</i>	<i>32° 52' 40.22''S</i>	<i>68° 55' 20.98''W</i>	<i>-5.18</i>	<i>-3.0</i>	<i>0.655 ± 0.013^c</i>	<i>37 ± 4</i>	<i>1.7 ± 1.1</i>
(2)					-5.24	-2.508	0.656 ± 0.009		
					-5.12	-3.458	0.654 ± 0.007		
<i>NAC-30</i> (1)	<i>600</i>	<i>30</i>	<i>34° 02' 60.00''S</i>	<i>67° 54' 09.90''W</i>	<i>-5.54</i>	<i>-6.7</i>	<i>0.703 ± 0.014</i>	<i>25 ± 3</i>	<i>-4.4 ± 0.8</i>
(2)					-5.53	-6.825	0.729 ± 0.009		
(3)					-5.53	-6.909	0.696 ± 0.008		
					-5.55	-6.457	0.683 ± 0.009		
<i>NAC-50</i> (1)	<i>600</i>	<i>50</i>	<i>34° 02' 60.00''S</i>	<i>67° 54' 09.90''W</i>	<i>-6.01</i>	<i>-8.3</i>	<i>0.652 ± 0.013</i>	<i>38 ± 4</i>	<i>-3.5 ± 0.7</i>
(2)					-5.53	-9.1	0.654 ± 0.009		
(3)					-6.09	-9.0	0.685 ± 0.008		
(4)					-5.92	-7.9	0.620 ± 0.008		
(Kiel (1))					-5.83	-8.1	0.649 ± 0.008		
(Kiel (2))					-6.27	-8.1			
					-6.41	-7.6			
<i>NAC-85</i> (1)	<i>600</i>	<i>85</i>	<i>34° 02' 60.00''S</i>	<i>67° 54' 09.90''W</i>	<i>-5.67</i>	<i>-7.6</i>	<i>0.695 ± 0.011^c</i>	<i>27 ± 3</i>	<i>-4.8 ± 0.5</i>
(2)					-5.58	-7.3	0.711 ± 0.008		
(3)					-5.60	-8.3	0.690 ± 0.009		
(Kiel (1))					-5.92	-7.0	0.684 ± 0.009		
(Kiel (2))					-5.60	-7.7			
					-5.63	-7.4			
<i>NAC-100</i> (1)	<i>600</i>	<i>100</i>	<i>34° 02' 60.00''S</i>	<i>67° 54' 09.90''W</i>	<i>-5.53</i>	<i>-8.5</i>	<i>0.678 ± 0.013^c</i>	<i>31 ± 3</i>	<i>-4.9 ± 0.9</i>
(2)					-5.49	-8.2	0.679 ± 0.008		
(3) ^t					-5.56	-8.8	0.677 ± 0.008		
					-6.10	-7.9			

Mean carbonate $\delta^{13}\text{C}$, $\delta^{18}\text{O}$, and Δ_{47} are reported for all sample analyses (bold, italicized). Below each sample summary, individual replicates for each sample are reported. Δ_{47} and 1SE are given for each individual replicate, but errors are not propagated to $T(\Delta_{47})$ and soil water $\delta^{18}\text{O}$ is not calculated.

^a Carbonate $\delta^{13}\text{C}$, $\delta^{18}\text{O}$, reported as mean and Δ_{47} reported as weighted mean of replicates (n) for each individual sample. Average external error (1SE) for replicates of a sample is $\pm 0.03\text{‰}$ for $\delta^{13}\text{C}$, $\pm 0.028\text{‰}$ for $\delta^{18}\text{O}$, and $\pm 0.019\text{‰}$ for Δ_{47} .

^b Soil water $\delta^{18}\text{O}$ was calculated using the calcite-water O-isotope fractionation equation of Kim and O'Neil (1997). Uncertainty in soil water $\delta^{18}\text{O}$ was calculated by propagating errors in $T(\Delta_{47})$.

^c For samples with fortuitously low SE for replicates, SE was assigned using the long-term SD of a standard run during the same period of time divided by \sqrt{n} , where n is the number of sample replicates, following Peters et al. (2013) and Huntington et al. (2009).

^t Samples with anomalous mass-48 values (exceeding those measured for heated CO_2 gases by $>1\text{‰}$) were rejected and are not reported in text or included in calculations.

Table B2 : Statistical comparison of $T(\Delta_{47})$ values

	<i>Passes standard t-test?</i>		
<i>Sites:</i>	CAN02	DL01	Nacuñan
CAN01	No $t(8) = 3.13, p = 0.02$	Yes $t(5) = 0.51, p = 0.63$	Yes $t(5) = 1.28, p = 0.23$
CAN02		Yes $t(4) = 1.37, p = 0.24$	Yes $t(4) = 0.58, p = 0.59$
DL01			Yes $t(6) = 0.61, p = 0.57$
	<i>Passes ANOVA test?</i>		
All four sites	Yes, $F(3, 17) = 5.43, p = 0.12$		

References

- Amundson, R., Wang, Y., Chadwick, O., Trumbore, S., McFadden, L., McDonald, E., Wells, S., and DeNiro, M., 1993. Factors and processes governing the ^{14}C content of carbonate in desert soils. *Earth and Planetary Science Letters*, v. 125, p. 385-405.
- Birkeland, P.W., 1999. *Soils and Geomorphology*. New York, Oxford University Press, 430 p.
- Breecker, D.O., Sharp, Z.D., and McFadden, L.D., 2009. Seasonal bias in the formation and stable isotopic composition of pedogenic carbonate in modern soils from central New Mexico, USA. *Geological Society of America Bulletin*, v. 121, no. 3-4, p. 630-640.
- Brocca, L., Camici, S., Melone, F., Moramarco, T., Martínez-Fernández, J., Didon-Lescot, J.-F., and Morbidelli, R., 2014. Improving the representation of soil moisture by using a semi-analytical infiltration model. *Hydrological Processes*, v. 28, p. 2103-2115.
- Brocca, L., Melone, F., and Moramarco, T., 2008. On the estimation of antecedent wetness conditions in rainfall-runoff modelling. *Hydrological Processes*, v. 22, p. 629-642.
- Caravagno, J.N., 1988. Distribution of C_3 and C_4 grasses at different altitudes in a temperate arid region of Argentina. *Oecologia*, v. 76, p. 273-277.
- Cerling, T.E., and Quade, J., 1993. Stable carbon and oxygen isotopes in soil carbonates, in Swart, P.K., Lohmann, K.C., McKenzie, J., and Savin, S.M., editors, *Climate change in continental isotopic records*, Geophysical Monograph: Washington D.C., American Geophysical Union, p. 217-231.
- Dennis, K.J., Affek, H.P., Passey, B.H., Schrag, D.P., and Eiler, J.M., 2011. Defining an absolute reference frame for 'clumped' isotope studies of CO_2 . *Geochimica et Cosmochimica Acta*, v. 75, p. 7117-7131.
- Drever, J.I., 1982. *The geochemistry of natural waters*. New York, Prentice Hall, 436p.

- Eiler, J.M., 2007. "Clumped-isotope" geochemistry-- The study of naturally-occurring, multiply substituted isotopologues. *Earth and Planetary Science Letters*, v. 262, p. 209-327.
- Friedman, I., and O'Neil, J.R., 1977. *Compilation of stable isotope fractionation factors of geochemical interest*. v. 400. US. GPO.
- Gabitov, R.I., Watson, E.B., and Sadekov, A., 2012. Oxygen isotope fractionation between calcite and fluid as a function of growth rate and temperature: An in situ study. *Chemical Geology*, v. 306-307, p. 92-102.
- Ghosh, P., Adkins, J., Affek, H., Balta, B., Guo, Wl., Schauble, E.A., Schrag, D., and Eiler, J.M., 2006. ^{13}C - ^{18}O bonds in carbonate minerals: A new kind of paleothermometer. *Geochimica et Cosmochimica Acta*, v. 70, p. 1430-1456.
- Ghosh, P., Garziane, C.N., and Eiler, J.M., 2006. Rapid uplift of the Altiplano revealed through ^{13}C - ^{18}O bonds in paleosol carbonates. *Science*, v. 311, p. 511-515.
- Gile, L.H., Peterson, F.F., and Grossman, R.B., 1966. Morphological and genetic sequences of carbonate accumulation in desert soils. *Soil Science*, v. 101, no. 5, p. 347-360.
- Guo, W., 2008. Carbonate clumped isotope thermometry: application to carbonaceous chondrites and effects of kinetic isotope fractionation. Dissertation, California Institute of Technology.
- Hoke, G.D., Aranibar, J.N., Viale, M., Araneo, D.C., and Llano, C., 2013. Seasonal moisture sources and the isotopic composition of precipitation, rivers, and carbonates across the Andes at 32.5 - 35.5°S. *Geochemistry, Geophysics, Geosystems*, v. 14, p. 962-978.
- Hoke, G.D., Garziane, C.N., Araneo, D.C., Latorre, C., Strecker, M.R., and Williams, K.J., 2009. The stable isotope altimeter: do quaternary pedogenic carbonates predict modern elevations? *Geology*, v. 37, p. 1015-1018.

- Hough, C.G., Fan, M., and Passey, B.H., 2013. Calibration of the clumped isotope geothermometer in soil carbonate in Wyoming and Nebraska, USA: Implications for paleoelevation and paleoclimate reconstruction. *Earth and Planetary Science Letters*, v. 391, p. 110-120.
- Huntington, K.W., Eiler, J.M., Affek, H.P., Guo, W., Bonifacie, M., Yeung, L.Y., Thiagarajan, N., Passey, B., Tripathi, A., Daeron, M., and Came, R., 2009. Methods and limitation of 'clumped' CO₂ isotope (D₄₇) analysis by gas-source isotope ratio mass spectrometry. *Journal Mass Spectrometry*, v. 44, p. 1318-1329.
- Jobbagy, E.G. and Jackson, R.B., 2001. The distribution of soil nutrients with depth: Global patterns and the imprint of plants. *Biogeochemistry*, v. 53, p. 51-77.
- Kim, S., and O'Neil, J.R., 1997. Equilibrium and nonequilibrium oxygen isotope effects in synthetic carbonates. *Geochimica et Cosmochimica Acta*, v. 61, p. 3461-3475.
- Lisiecki, L. E., Raymo, M. E., 2005. A Pliocene-Pleistocene stack of 57 globally distributed benthic d₁₈O records. *Paleoceanography*, v. 20, PA1003, doi:10.1029/2004PA001071.
- Meyer, N.A., Breecker, D.O., Young, M.H., Litvak, M.E., 2014. Simulating the effect of vegetation in formation of pedogenic carbonate. *Pedology, Soil Science Society of America Journal*, v. 78, p. 914-924.
- Ojeda, R.A., Campos, C.M., Gonnet, J.M., Borghi, C.E., and Roig, V.G., 1998. The MaB Reserve of Ñacuñán, Argentina: its role in understanding the Monte Desert biome. *Journal of Arid Environments*, v.39, p. 299-313.
- Passey, B.H. and Henkes, G.A., 2012. Carbonate clumped isotope bond reordering and geospeedometry. *Earth and Planetary Science Letters*, v. 351-352, p. 223-236.

Passey, B.H., Levin, N.E., Cerling, T.E., Brown, F.H., Eiler, J.M., and Turekian, K.K., 2010.

High-temperature environments of human evolution in East Africa based on bond ordering in paleosol carbonates. *Proceedings of the National Academy of Sciences of the United States of America*, v. 107, p. 11245-11249.

Peters, N.A., Huntington, K.W., and Hoke, G.D., 2013. Hot or not? Impact of seasonally variable soil carbonate formation on paleotemperature and O-isotope records from clumped isotope thermometry. *Earth and Planetary Science Letters*.

<http://dx.doi.org/10.1016/j.epsl.2012.10.024>

Plummer, L.N. and Busenberg, E., 1982. The solubilities of calcite, aragonite and vaterite in CO₂-H₂O solutions between 0 and 90°C, and an evaluation of the aqueous model for the system CaCO₃-CO₂-H₂O. *Geochimica et Cosmochimica Acta*, v. 46, p. 1011-1040.

Rossi, B.E., and Villagra, P.E., 2003. Effects of *Prosopis flexuosa* on soil properties and the spatial pattern of understorey species in arid Argentina. *Journal of Vegetation Science*, v. 14, p. 543-550.

Rossi, B.E., 2004. Flora y vegetación de la Reserva de Biosfera de Nacuñán después de 25 años de clausura. Ph.D. thesis. la Universidad Nacional de Córdoba, Córdoba, Argentina.

Quade, J., Garzione, C., and Eiler, J., 2007. Paleoelevation reconstruction using pedogenic carbonates. *Reviews in Mineralogy and Geochemistry*, v. 66, p. 53-87.

Quade, J., Eiler, J., Daeron, M., Achyuthan, H., 2013. The clumped isotope geothermometer in soil and paleosol carbonate. *Geochimica et Cosmochimica Acta*, v. 105, p. 92-107.

Schmidt, S., Hetzel, R., Mingoance, F., Ramos, V., 2011. Coseismic displacements and Holocene slip rates for two active thrust faults at the mountain front of the Andean Precordillera (~33°S). *Tectonics*, v. 30, TC5011.

- Yang, W., Amundson, R., and Trumbore, S., 1994. A model for soil $^{14}\text{CO}_2$ and its implications for using ^{14}C to date pedogenic carbonate. *Geochimica et Cosmochimica Acta*, v. 58, p. 393-399.
- Zaarur, S., Affek, H.P., and Brandon, M.T., 2013. A revised calibration of the clumped isotope thermometer. *Earth and Planetary Science Letters*, v. 382, p. 47-57.

Curriculum Vitae

Mallory Ringham

Department of Earth Sciences, Syracuse University
204 Heroy Geology Laboratory, Syracuse, NY 13244
315-200-5685 • mcringha@syr.edu

EDUCATION

Master of Science: Earth Sciences

Expected June 2015

Syracuse University, Syracuse, NY

Bachelor of Science: Physics and Chemical Engineering, minor in Mathematics May 2013

Syracuse University, Syracuse, NY

Summa cum laude, Renée Crown University Honors Program

EXPERIENCE AND RESEARCH

Hoke Laboratory, Department of Earth Sciences, Syracuse University

Graduate Research Assistant, Fall 2013-Spring 2015

- "Influence of environment on soil carbonate clumped isotope records, Andean piedmont of central Argentina (33-34°S)"; "Simulating the effect of seasonal precipitation on soil carbonate formation"; "Pleistocene climate records from soil carbonate clumped isotopes of Las Carreras loess-paleosol sequence, northwest Argentina (26°S)"

Teaching Assistant, EAR 105, Syracuse University, Earth Sciences Department

TA for EAR 105, Earth Sciences for non-majors, Fall 2013 & Fall 2014

Siegel Laboratory, Syracuse University Earth Sciences Department

Undergraduate Researcher, Fall 2012-Spring 2013

- "A Temporal Geochemical Characterization of Water Sources in the Lives of Storms"
- ICP-OES and Picarro stable hydrogen / oxygen isotope-based analysis of precipitation chemistry during winter storms in Upstate NY

Summer Student Fellow, Woods Hole Oceanographic Institution

Deep Submergence Laboratory Intern under the supervision of Dr. Chip Breier, Summer 2012

- "An Autonomous Sampler for Multi-time Scale River Chemistry Observations"

Maye Laboratory, Syracuse University Chemistry Department

Undergraduate Research Assistant, Fall 2011-Spring 2012

- Cyclic voltammetry study of methanol oxidation reactions with Ag/Au nanoparticle alloys

Bader Laboratory, Syracuse Biomaterials Institute, Syracuse University

Undergraduate Research Assistant, Spring 2010-Spring 2011

- Optimized synthesis of Polyethylene glycol-based beads for oral drug delivery applications

COMPUTER SKILLS:

MATLAB, LabVIEW, Maple, HYSPLIT, HYDRUS 1D, SHAW, COMSOL, ChemCAD